The University Of Queensland
AUSTRALIA
CREATE CHANGE

Optomechanical sensing

Dr Christopher Baker

EQUS Autumn School, Noosa, May 9th 2024

EQUS
Australian Research Council
Centre of Excellence for
Engineered Quantum Systems

Basics of resonant sensing

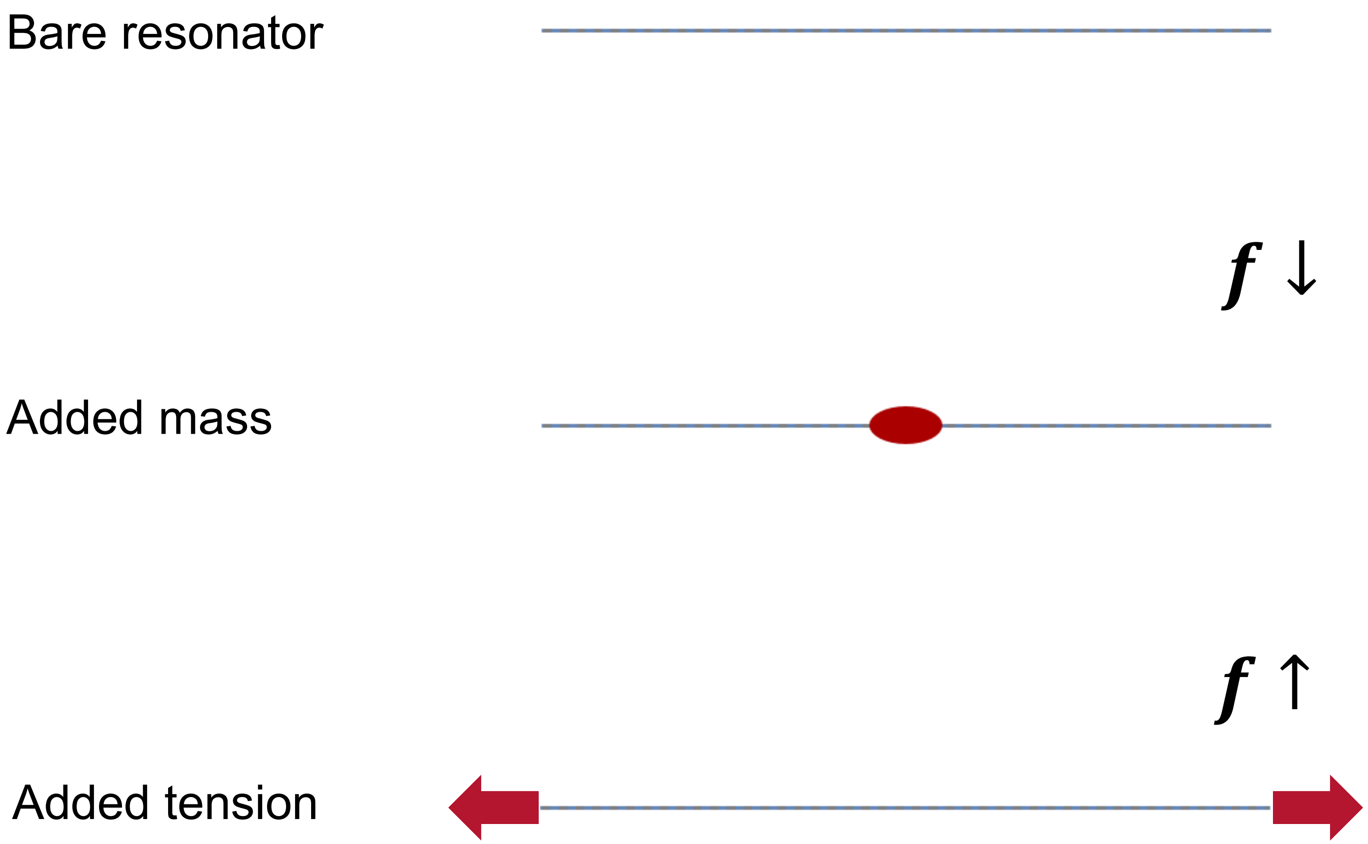

Resonant sensing

$$f_n = \sqrt{\frac{\sigma}{\rho}}\,\frac{n}{2L}$$

The resonance frequency of the string is sensitive to changes in density and tension

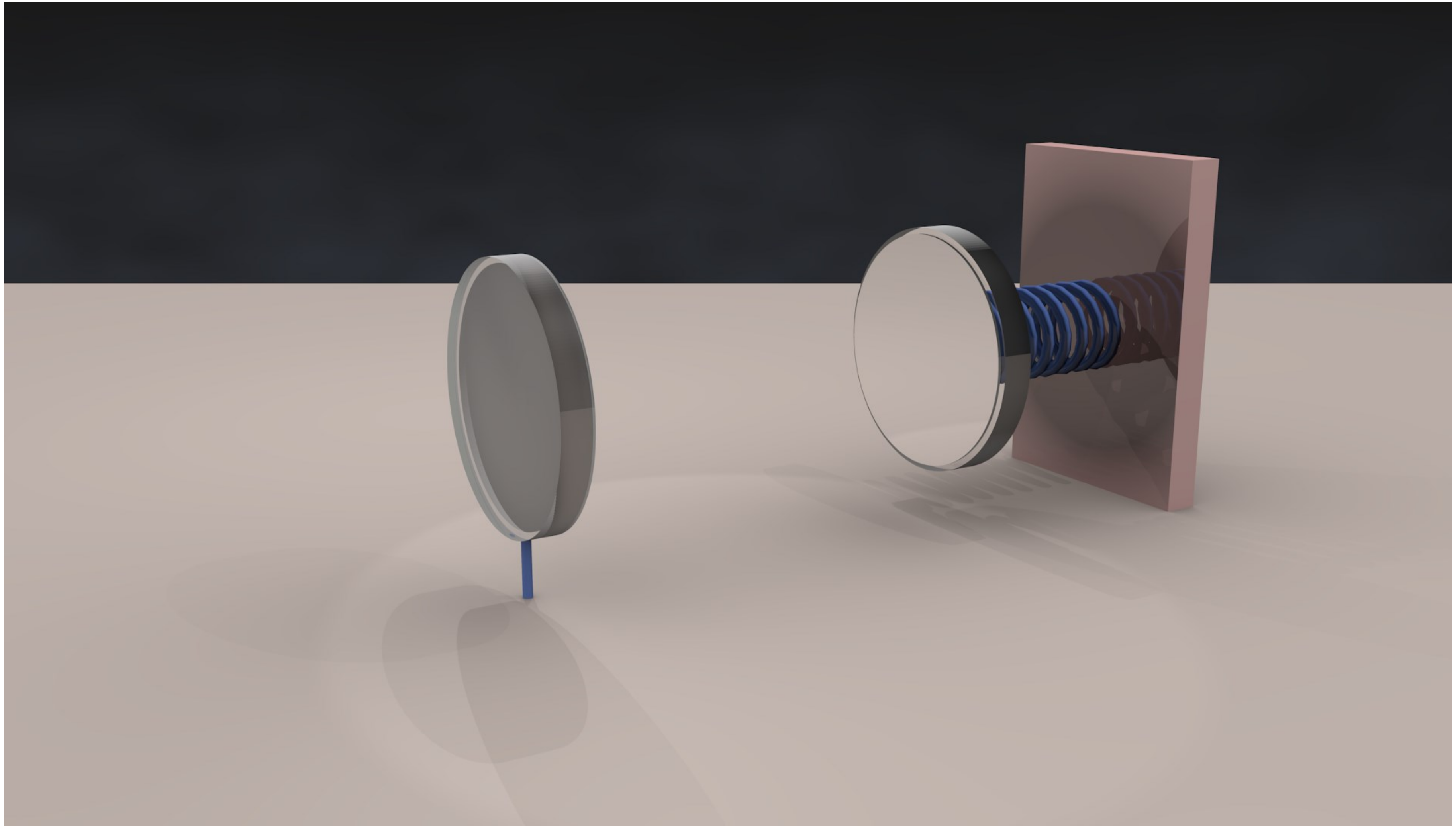

Mechanical element can be functionalized to be made to interact with a wide range of stimuli

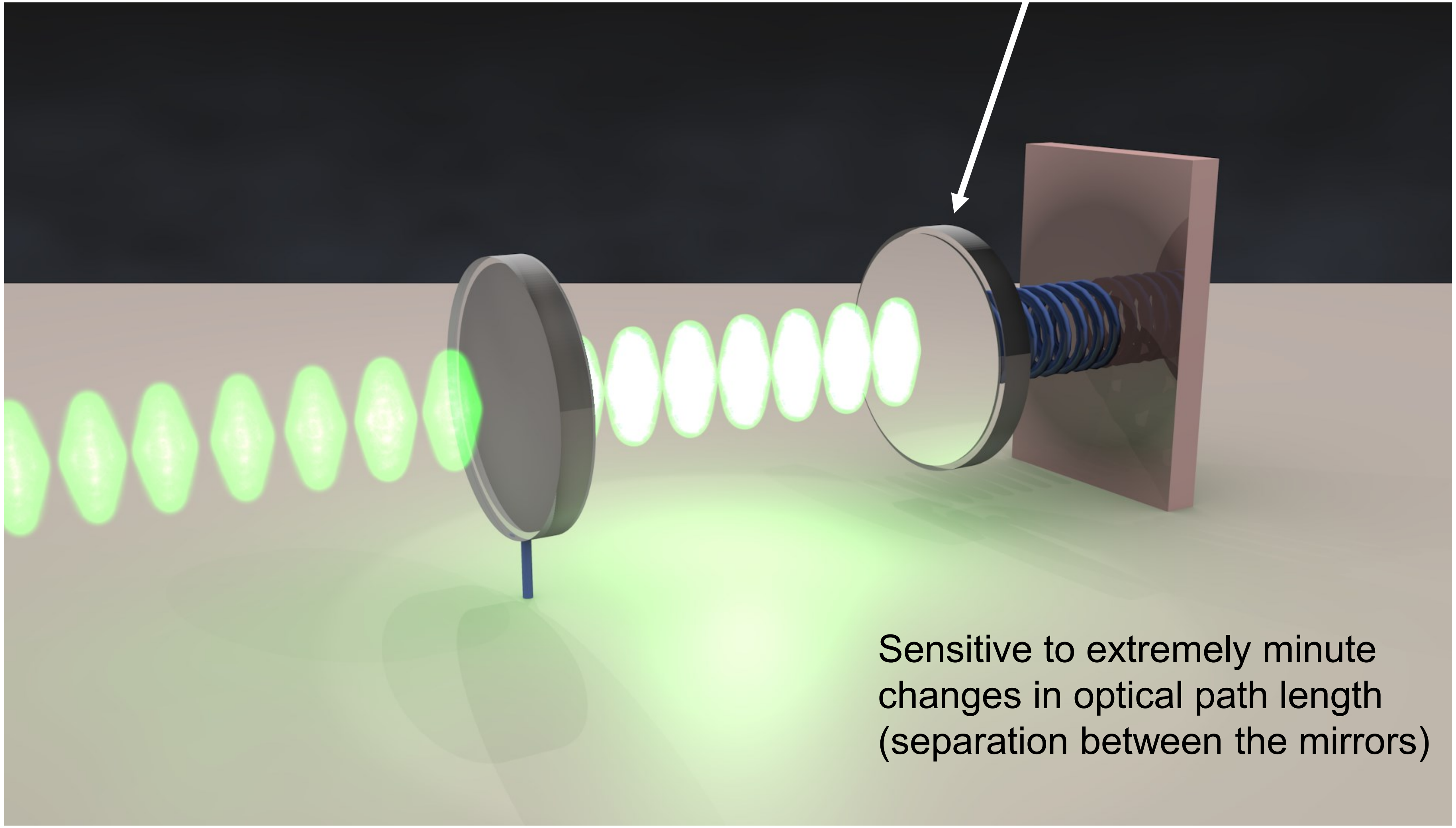

Optical resonators come in various forms

Fabry-Perot cavities

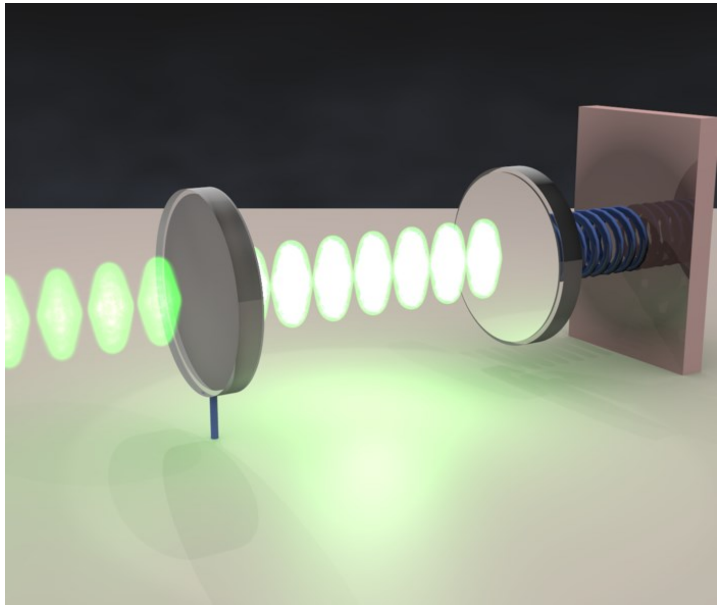

Whispering gallery mode (WGM) resonators

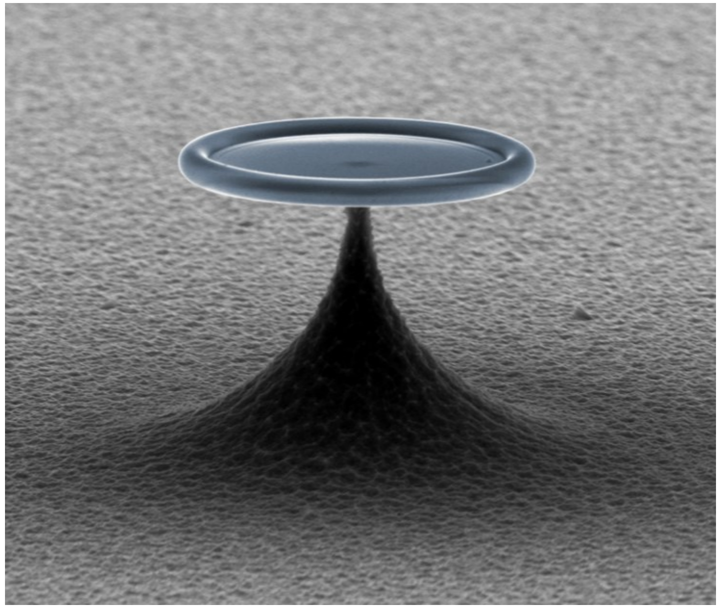

Photonic crystal cavities

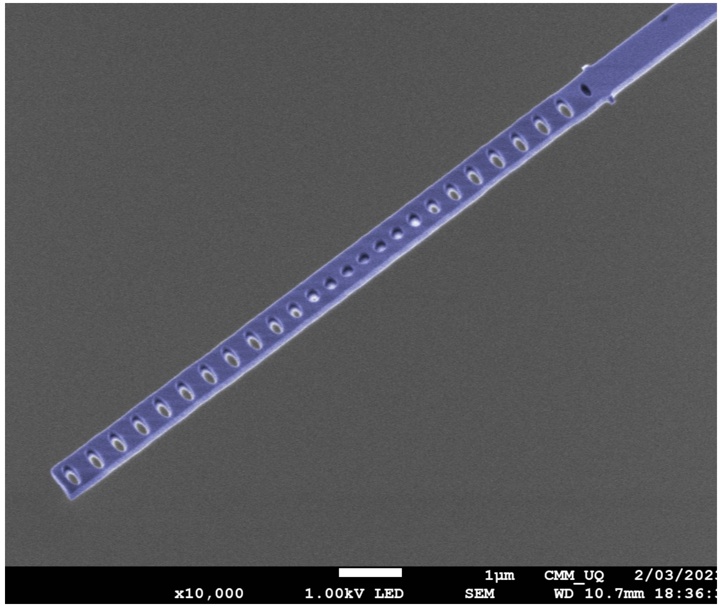

Photonic crystal

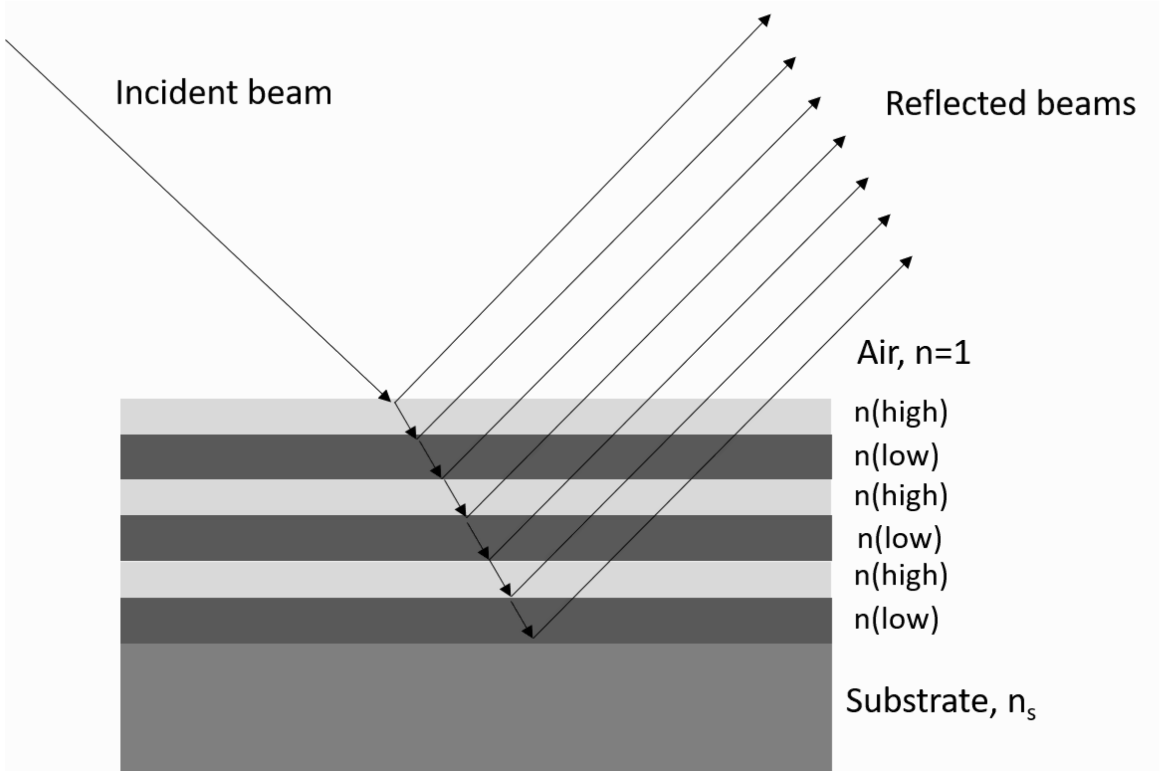

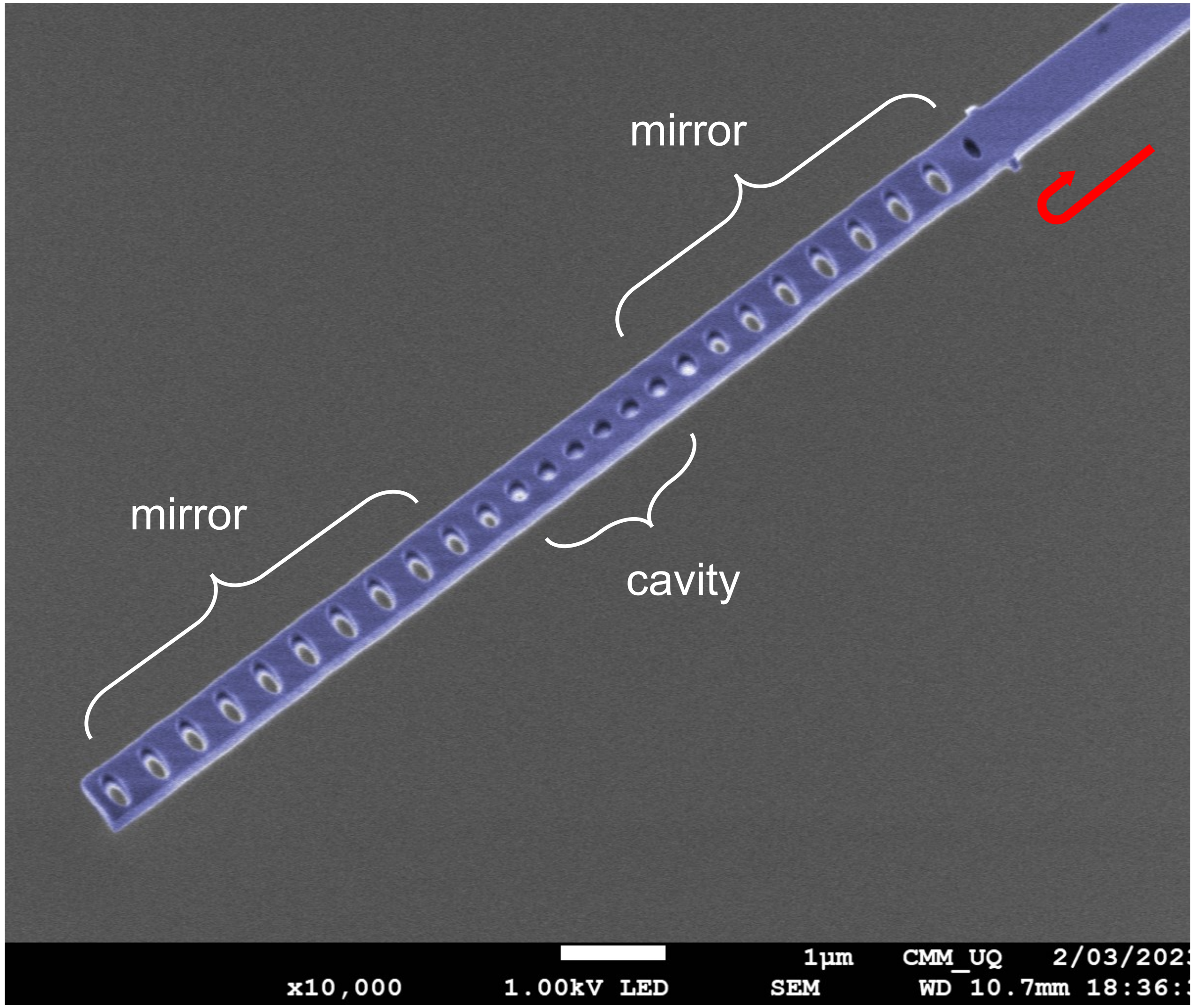

1D photonic crystal cavity

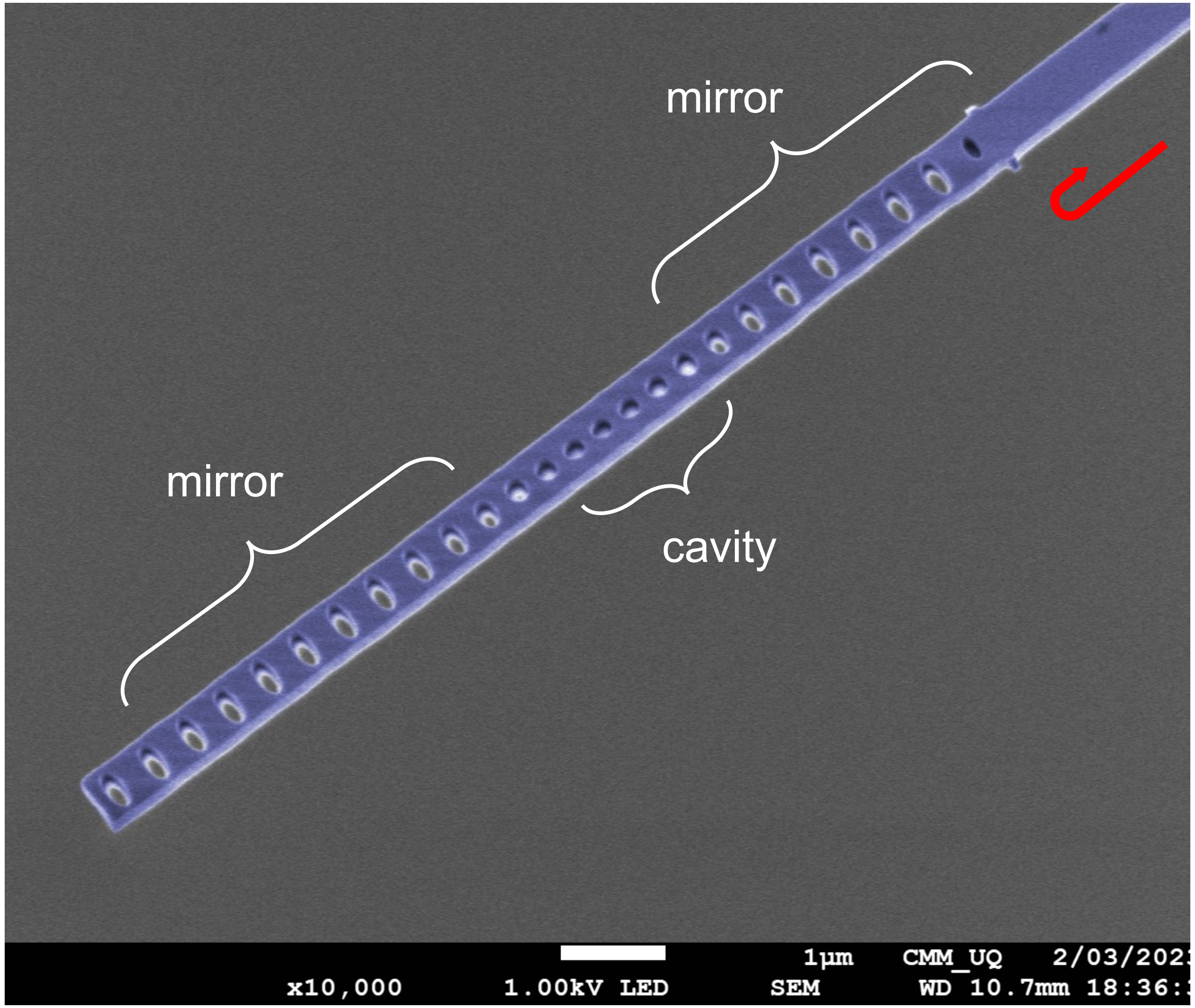

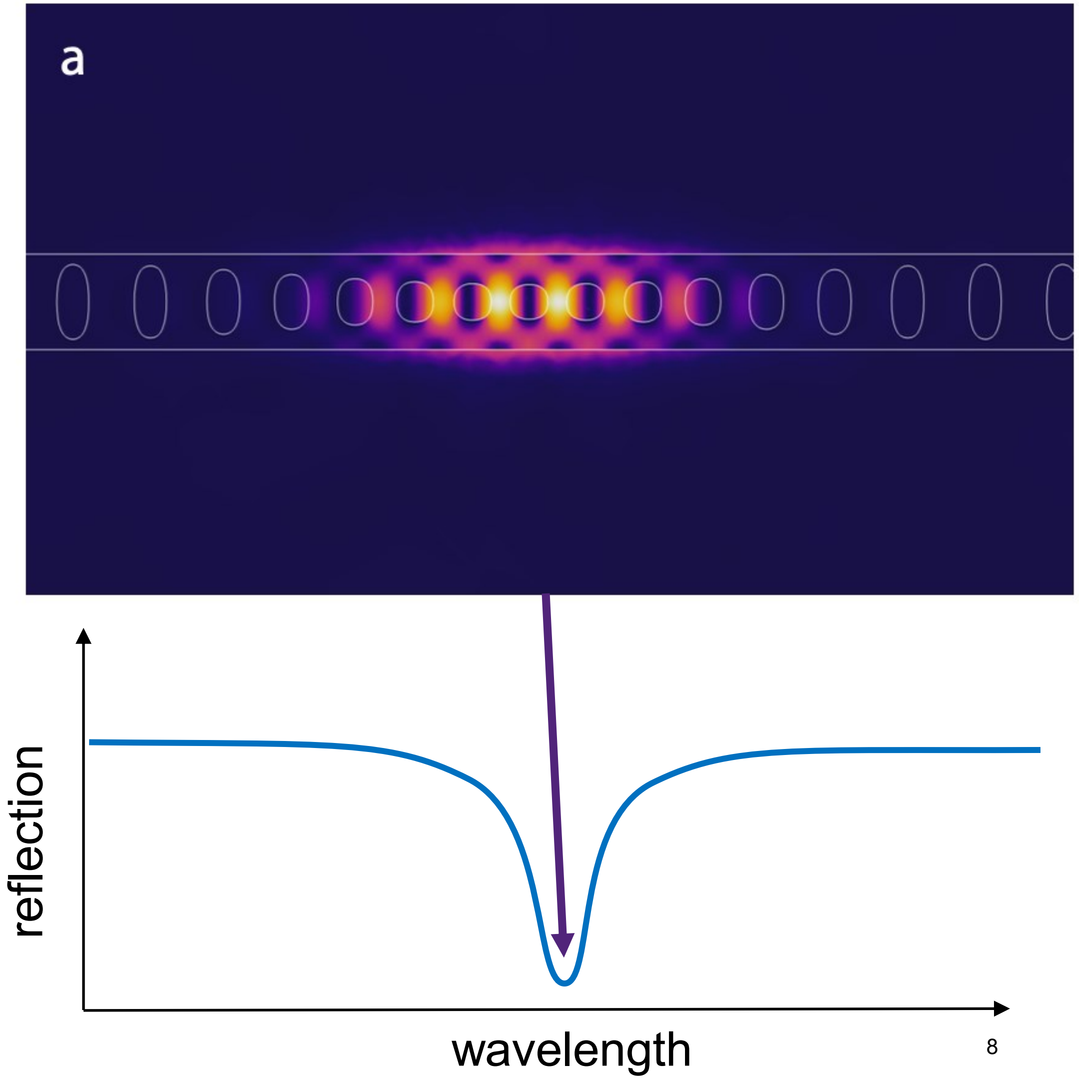

Whispering gallery mode resonators

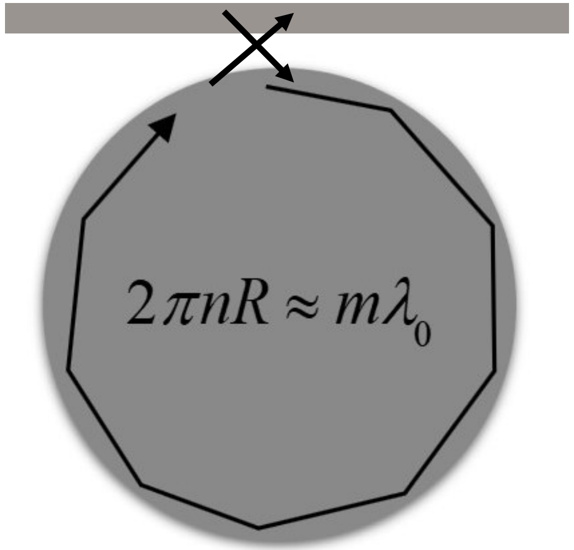

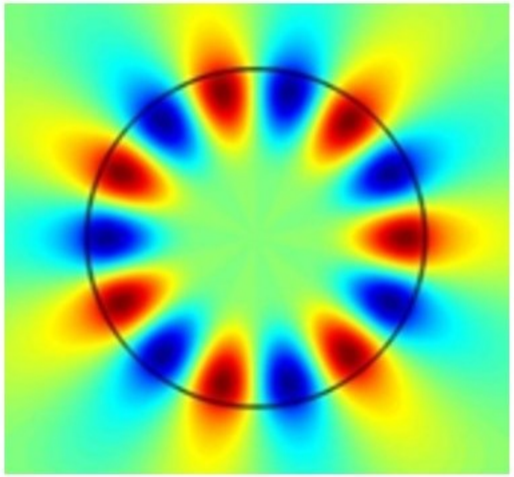

Whispering gallery mode resonators

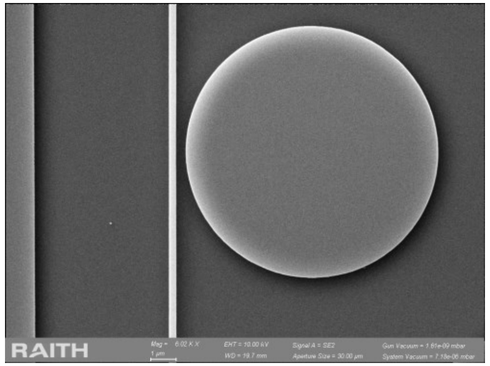

$$2\pi\, n_{\mathrm{eff}}\, R = m\lambda_0$$

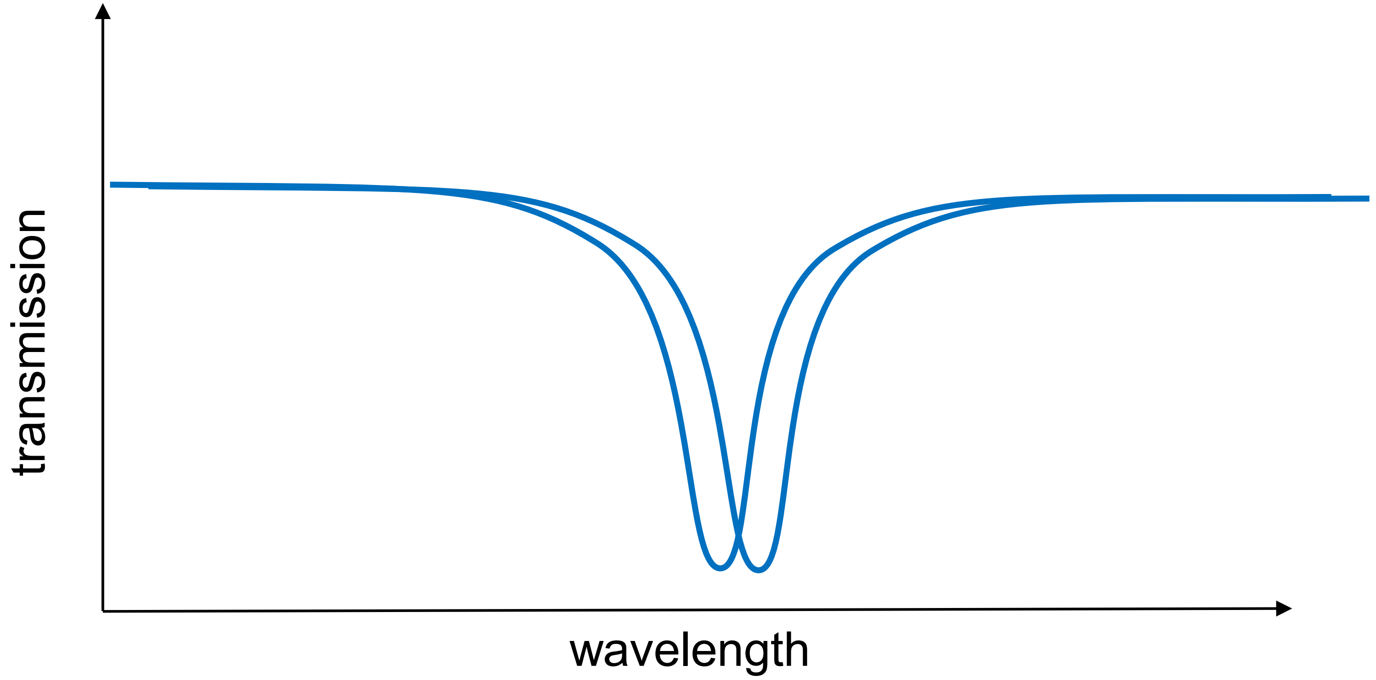

Force
Acceleration
Magnetic fields
Electric fields
Temperature
Gases
Ultrasounds
Gravitational waves
Viscosity
Biological particles…

Optical quality factor

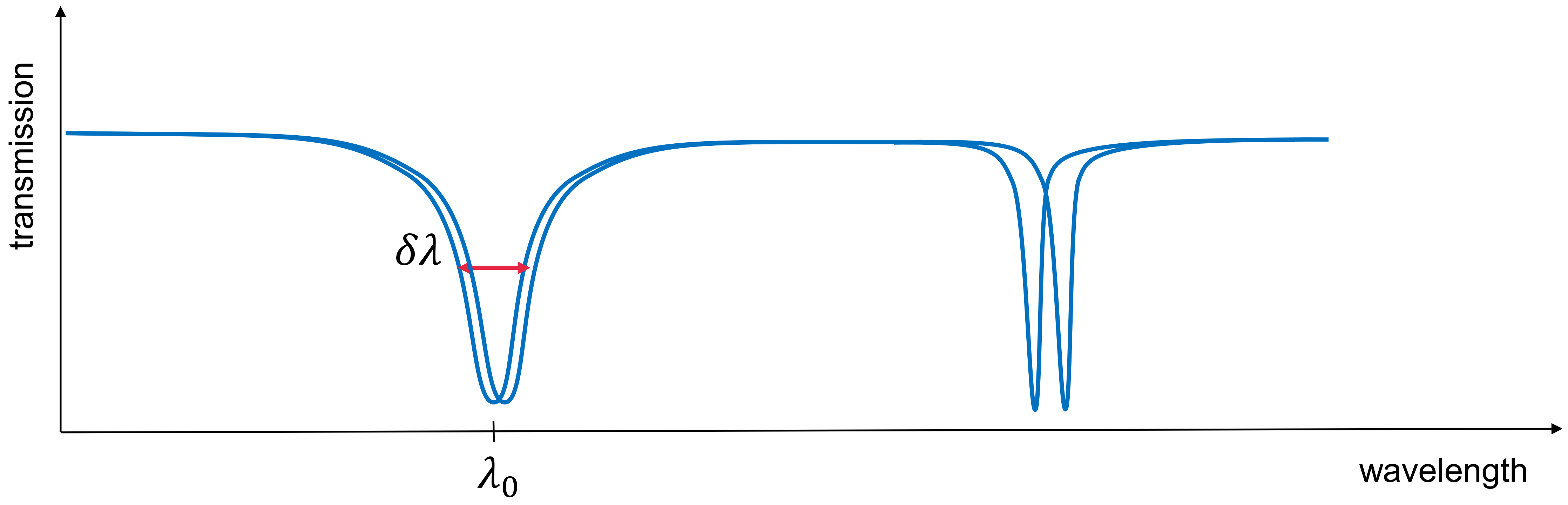

$$Q = \frac{\lambda_0}{\delta\lambda}$$

→ Higher optical Q leads to improved sensitivity

Optical quality factor

- Material absorption Choose low loss material
- Bending losses Use larger bend radius/ use higher refractive index material
- Surface losses Control surface state (piranha, HF treatments, ALD…)
- Sidewall roughness Multipass exposure, resist reflow…

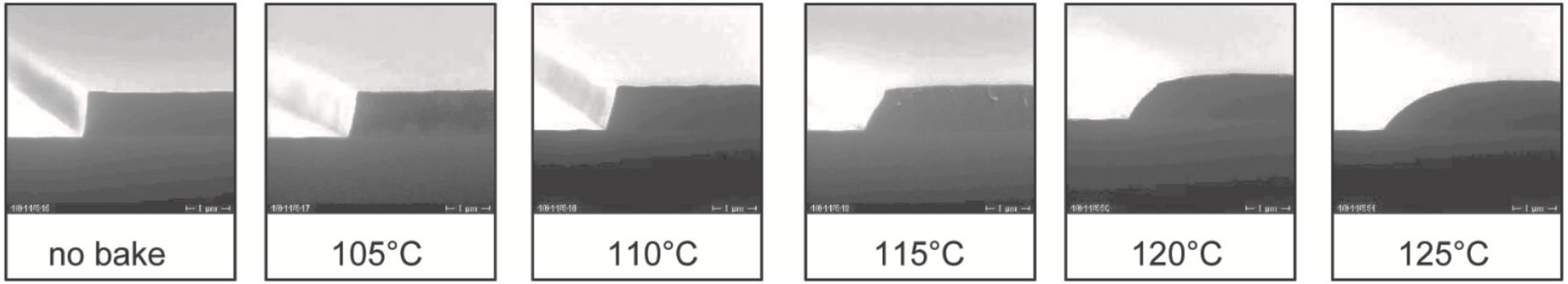

Cross-section of resist structures at increasing bake temperatures (AZ® ECI 3000). *Source: AZ-EM® AZ® ECI 3000 Product Data Sheet*

Material reflow

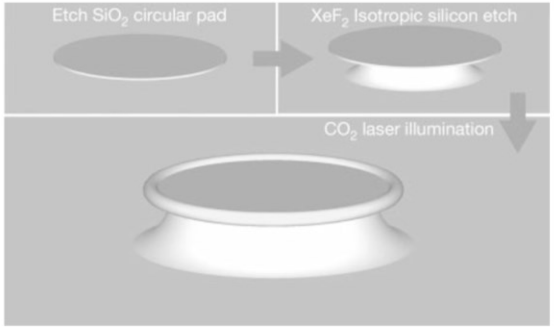

Figure 1 Flow diagram illustrating the process used to fabricate ultra-high-Q planar microcavities.

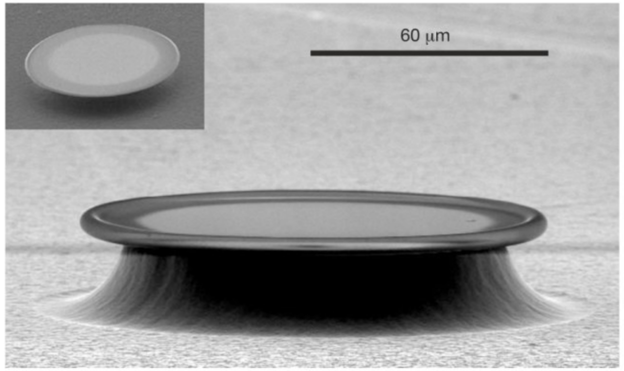

Figure 2 Scanning electron micrograph of a silica microdisk after selective reflow treatment with a CO_2 laser. The inset shows the microdisk prior to laser treatment. This toroidal microresonator had an intrinsic cavity Q of 1.00×10^8.

process. The circular disks of photo-resist act as an etch mask during immersion in buffered HF solution at room temperature. Acetone is

Armani, D. K., Kippenberg, T. J., Spillane, S. M. & Vahala, K. J. Ultra-high-Q toroid microcavity on a chip. *Nature* **421**, 925 (2003).

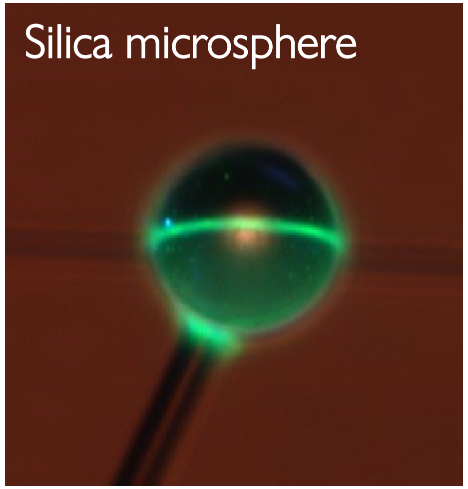

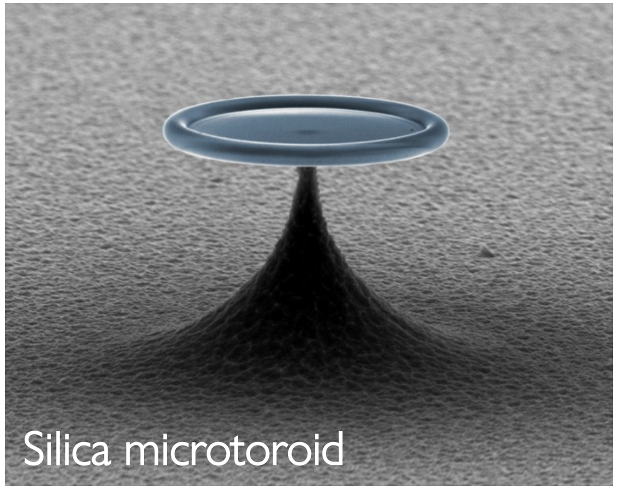

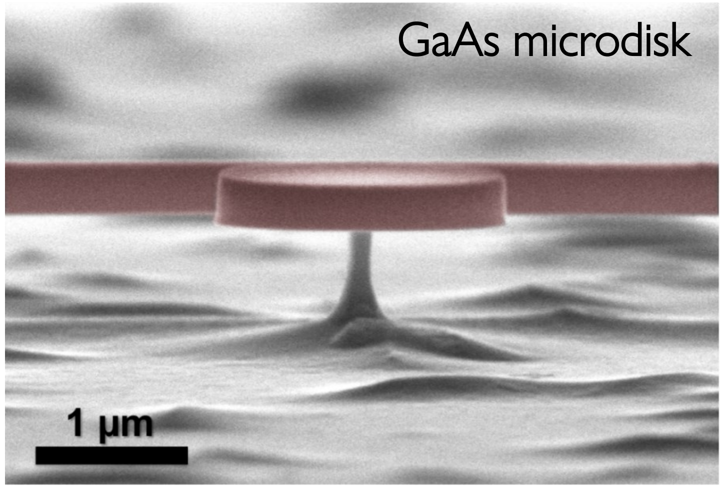

Sensors

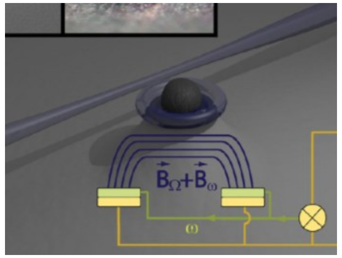

Magnetic fields

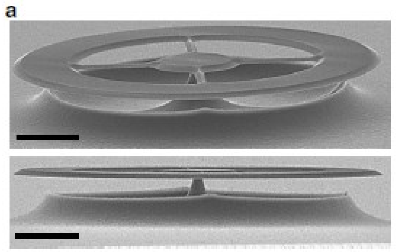

ultrasounds

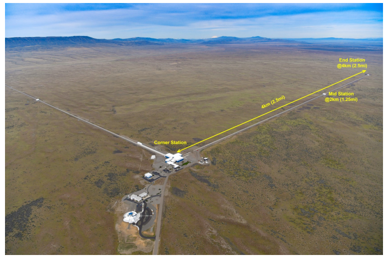

Gravitational waves

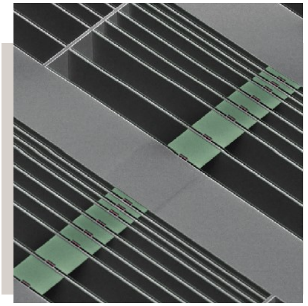

acceleration

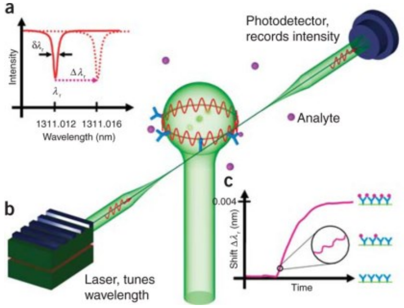

biosensors

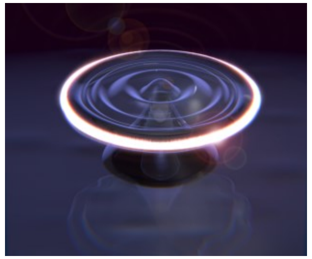

Superfluid waves


Signal
Change in optical path length
Readout

Why use a resonator?

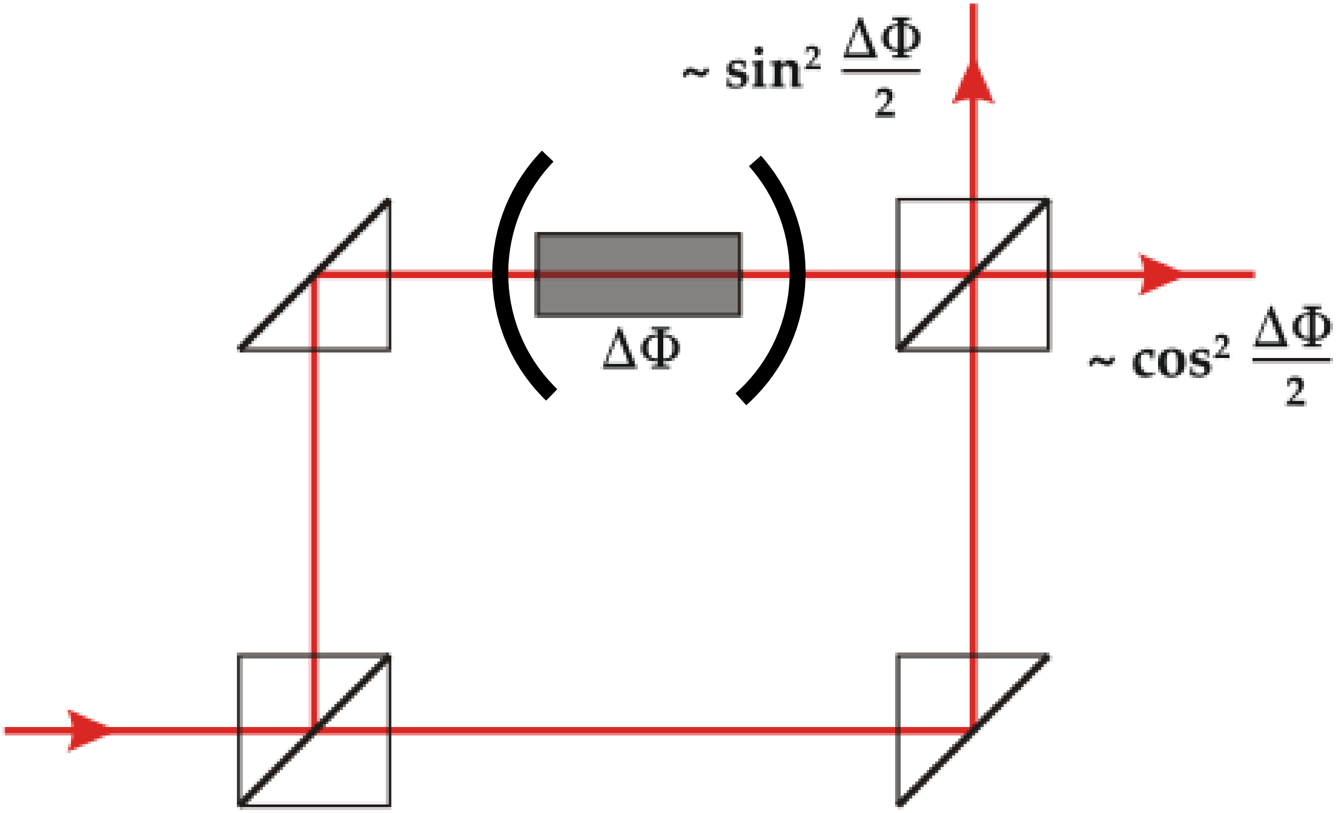

$$\Delta\Phi \rightarrow F\Delta\Phi$$

Gravitational waves

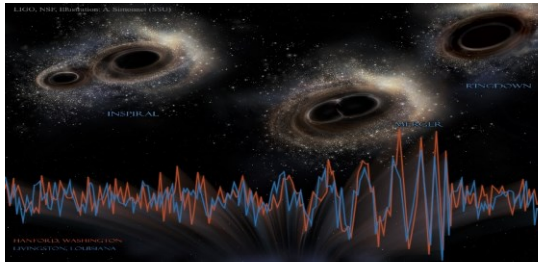

LIGO Scientific Collaboration and Virgo Collaboration *et al.*, "Observation of Gravitational Waves from a Binary Black Hole Merger," *Phys. Rev. Lett.*, vol. 116, no. 6, p. 061102, Feb. 2016.

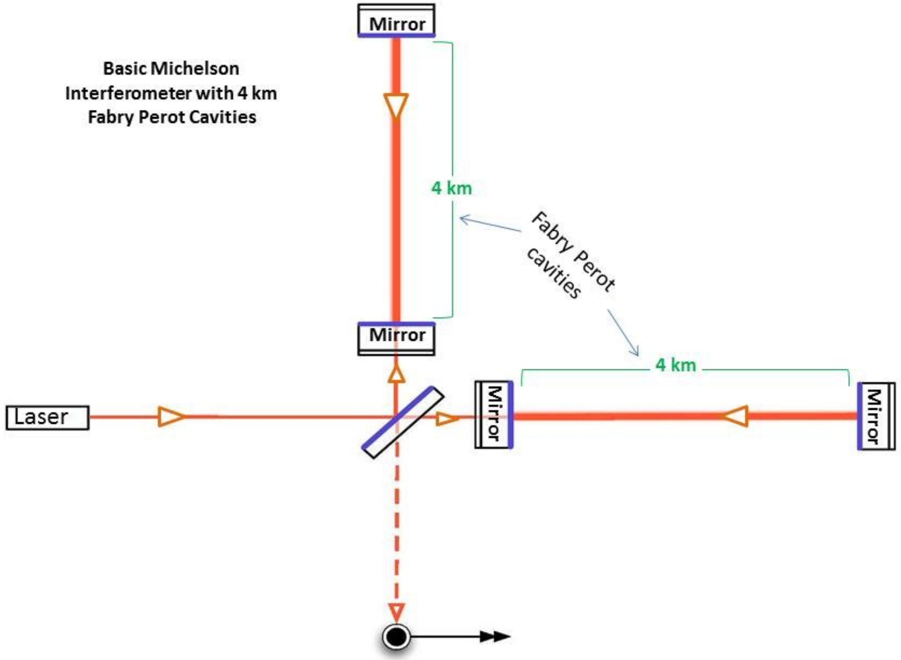

magnetometry

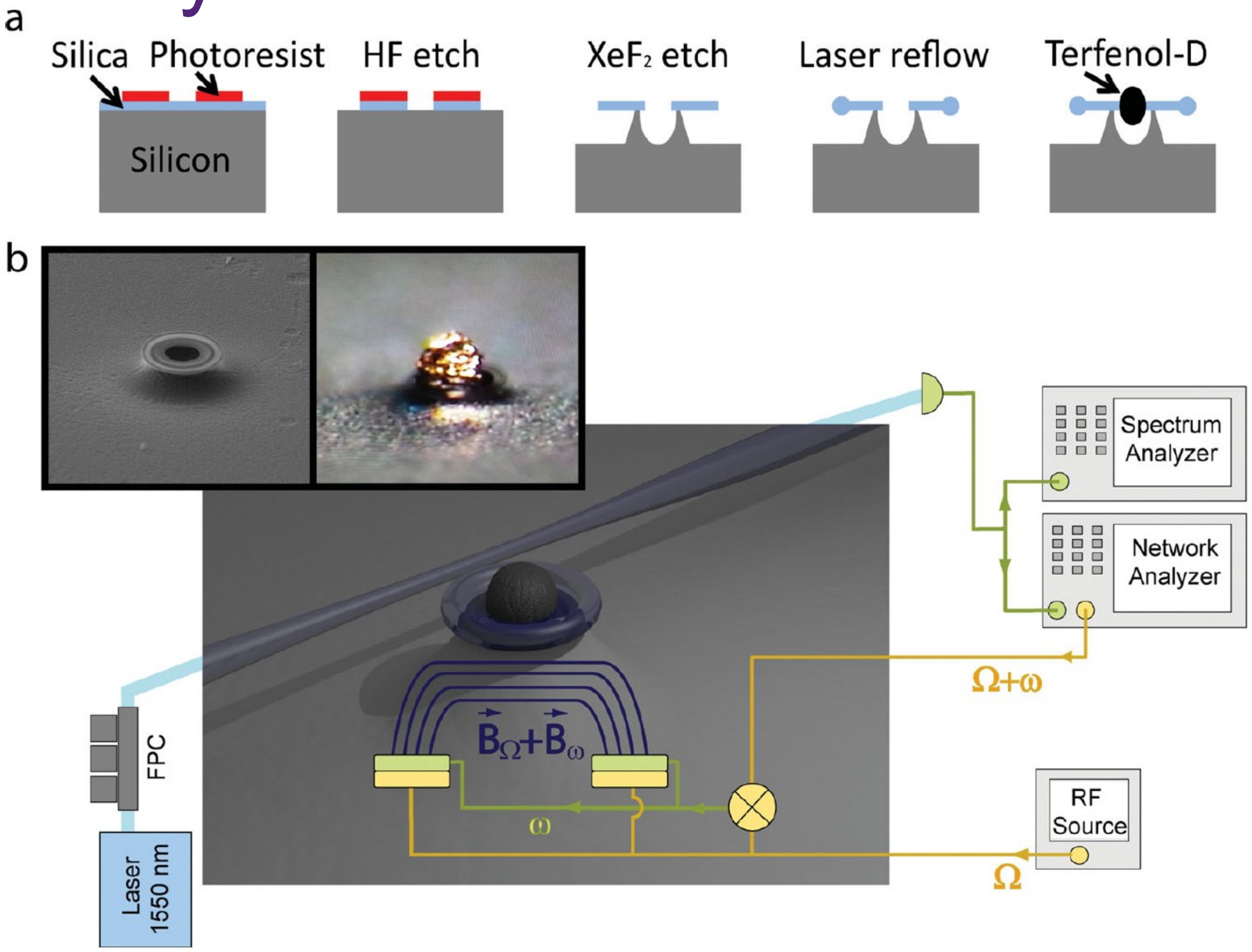

$$\frac{\Delta R}{R} = \frac{\Delta\lambda}{\lambda} = \frac{1}{Q} \rightarrow \Delta R = \frac{R}{Q}$$

→ With R=30um and Q=3x10^7
ΔR~0.01 Angstrom for linewidth shift

B.-B. Li, J. Bílek, U. B. Hoff, L. S. Madsen, S. Forstner, V. Prakash, C. Schäfermeier, T. Gehring, W. P. Bowen, and U. L. Andersen, *Quantum Enhanced Optomechanical Magnetometry*, Optica, OPTICA **5**, 850 (2018).
S. Forstner, S. Prams, J. Knittel, E. D. van Ooijen, J. D. Swaim, G. I. Harris, A. Szorkovszky, W. P. Bowen, and H. Rubinsztein-Dunlop, *Cavity Optomechanical Magnetometer*, Phys. Rev. Lett. **108**, 120801 (2012).
S. Forstner, E. Sheridan, J. Knittel, C. L. Humphreys, G. A. Brawley, H. Rubinsztein-Dunlop, and W. P. Bowen, *Ultrasensitive Optomechanical Magnetometry*, Adv. Mater. **26**, 6348 (2014).

accelerometry

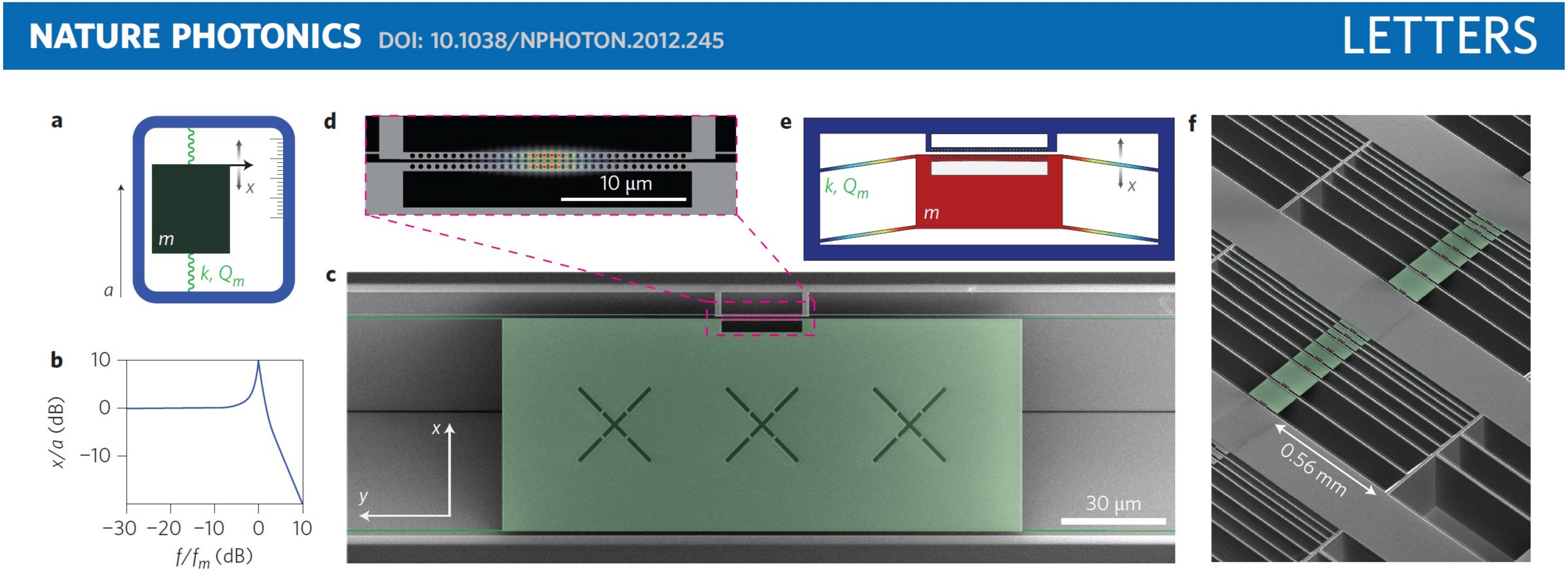

A. G. Krause, M. Winger, T. D. Blasius, Q. Lin, and O. Painter, *A High-Resolution Microchip Optomechanical Accelerometer*, Nat Photon **6**, 768 (2012).

Ultrasound sensing

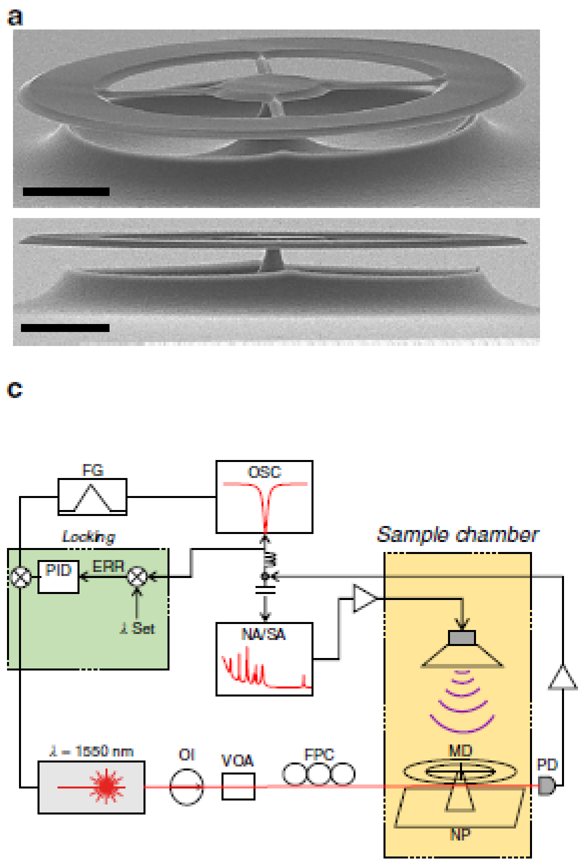

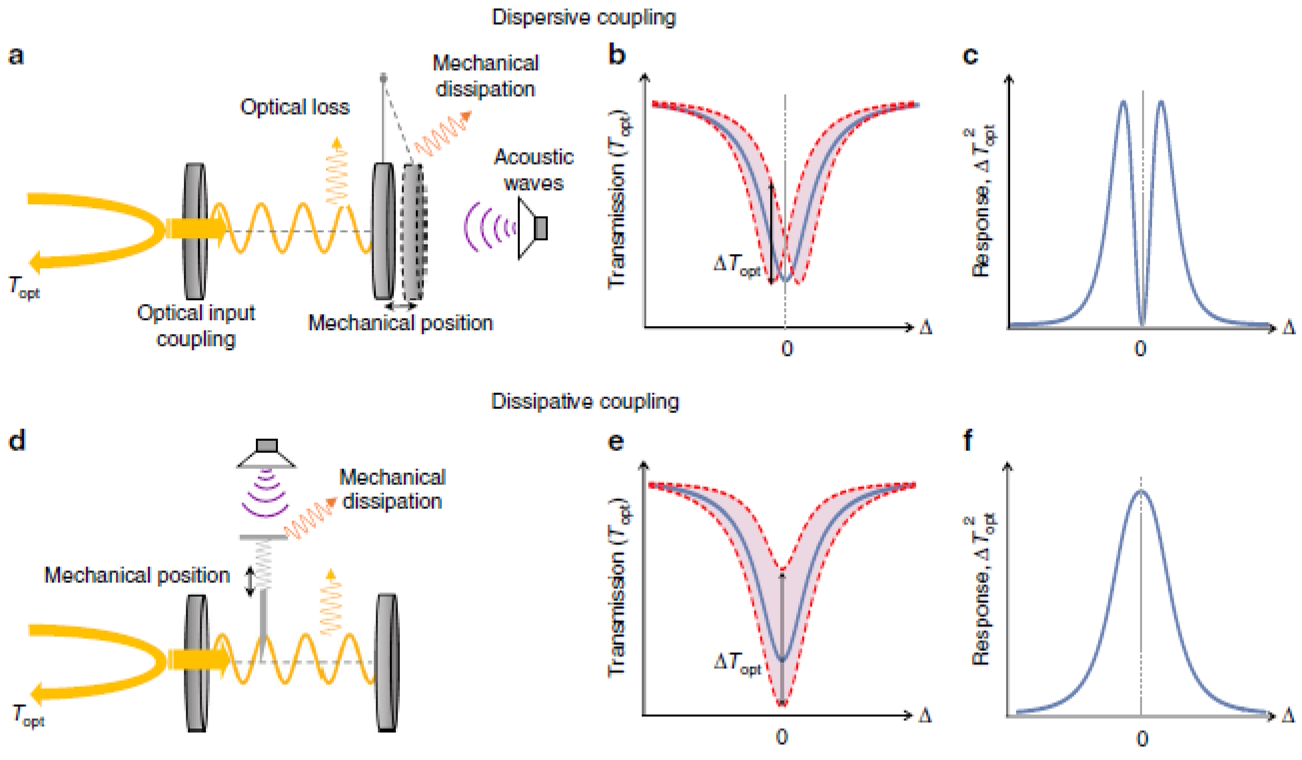

S. Basiri-Esfahani, A. Armin, S. Forstner, and W. P. Bowen, *Precision Ultrasound Sensing on a Chip*, Nature Communications **10**, 132 (2019).

Superfluid sensing

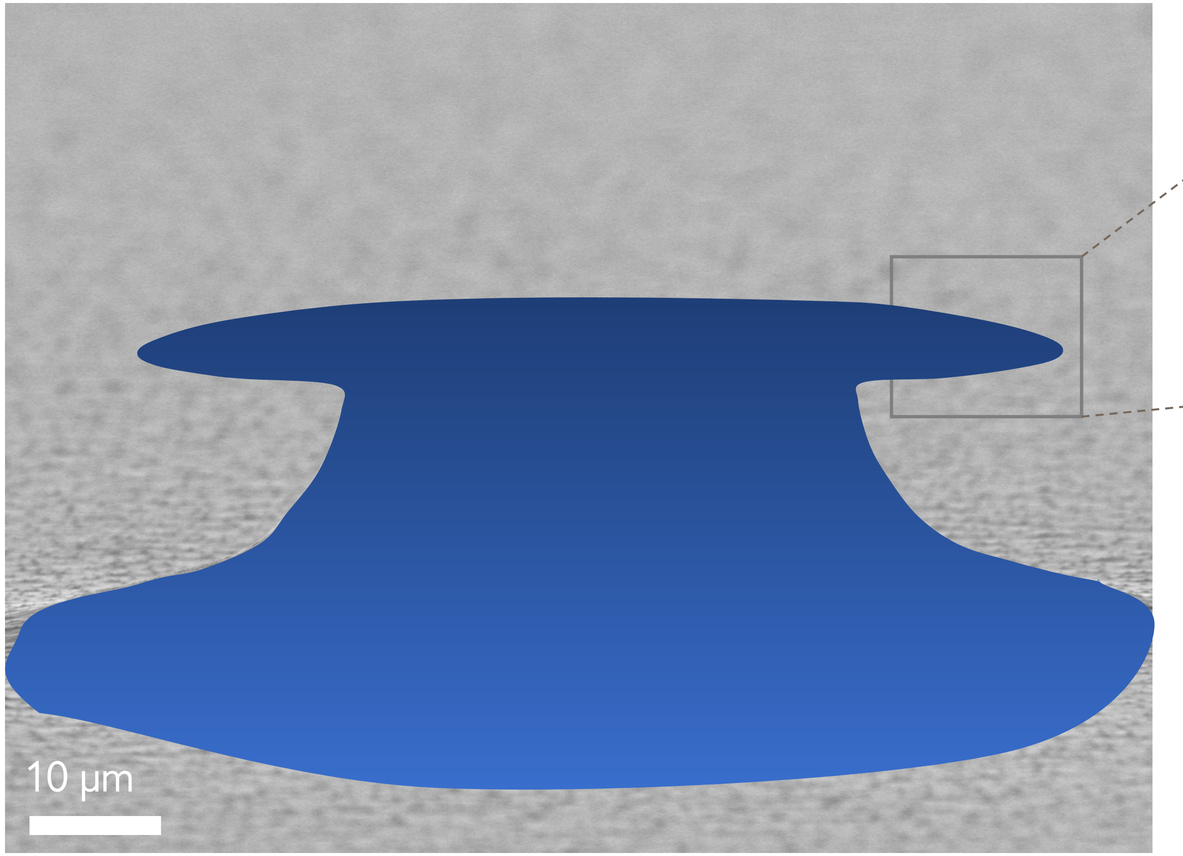

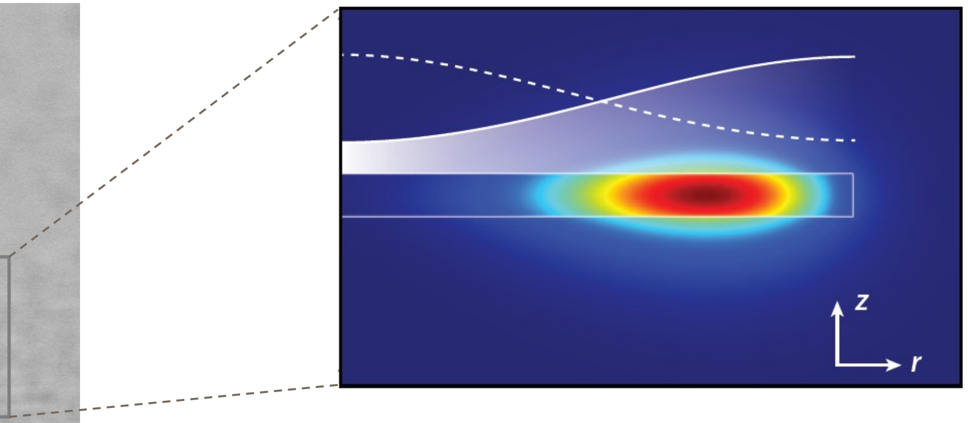

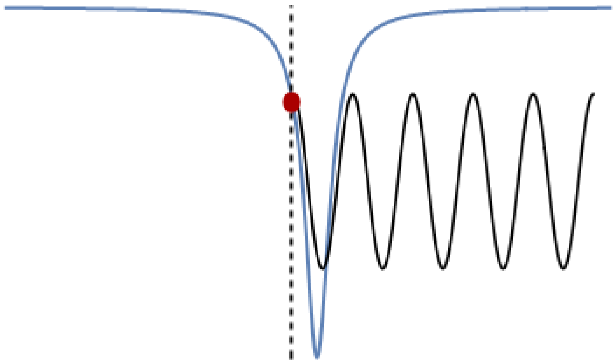

New Journal of Physics, 18(12):123025, 2016

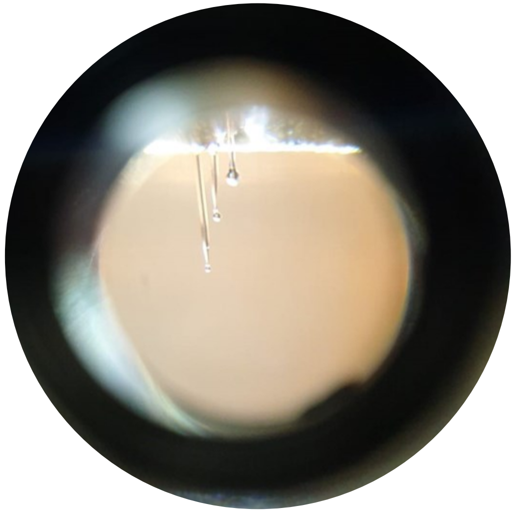

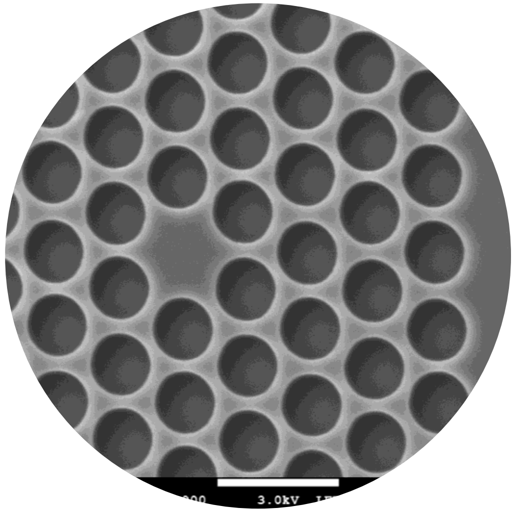

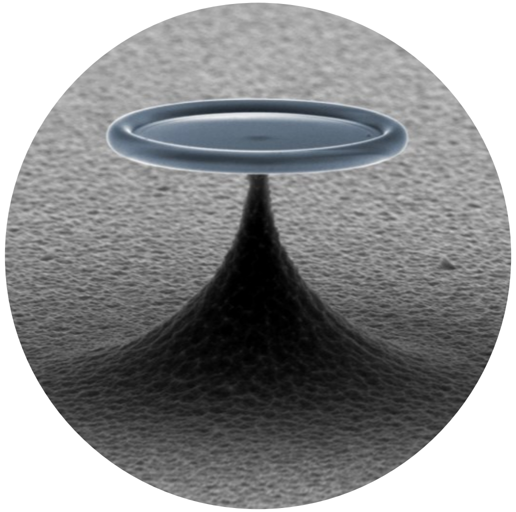

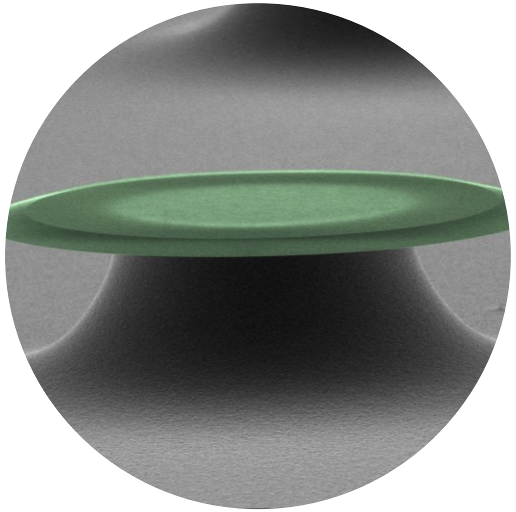

Nature Physics **12**, 788, 2016
Physical Review X, **6**:021012, 2016
New J. Phys. **18**, 123025, 2016.
New J. Phys. **21**, 053029, 2019.
Science **366**, 1480, 2019.

Nature Physics **16**, 4 2020.
*Optics Express, **28**, 22450 2020.*
Npj Quantum Information **7**, 1 2021.
*Optics Express, **30**, 30822 2022.*
*Science Advances **9** eade3591, 2023.*

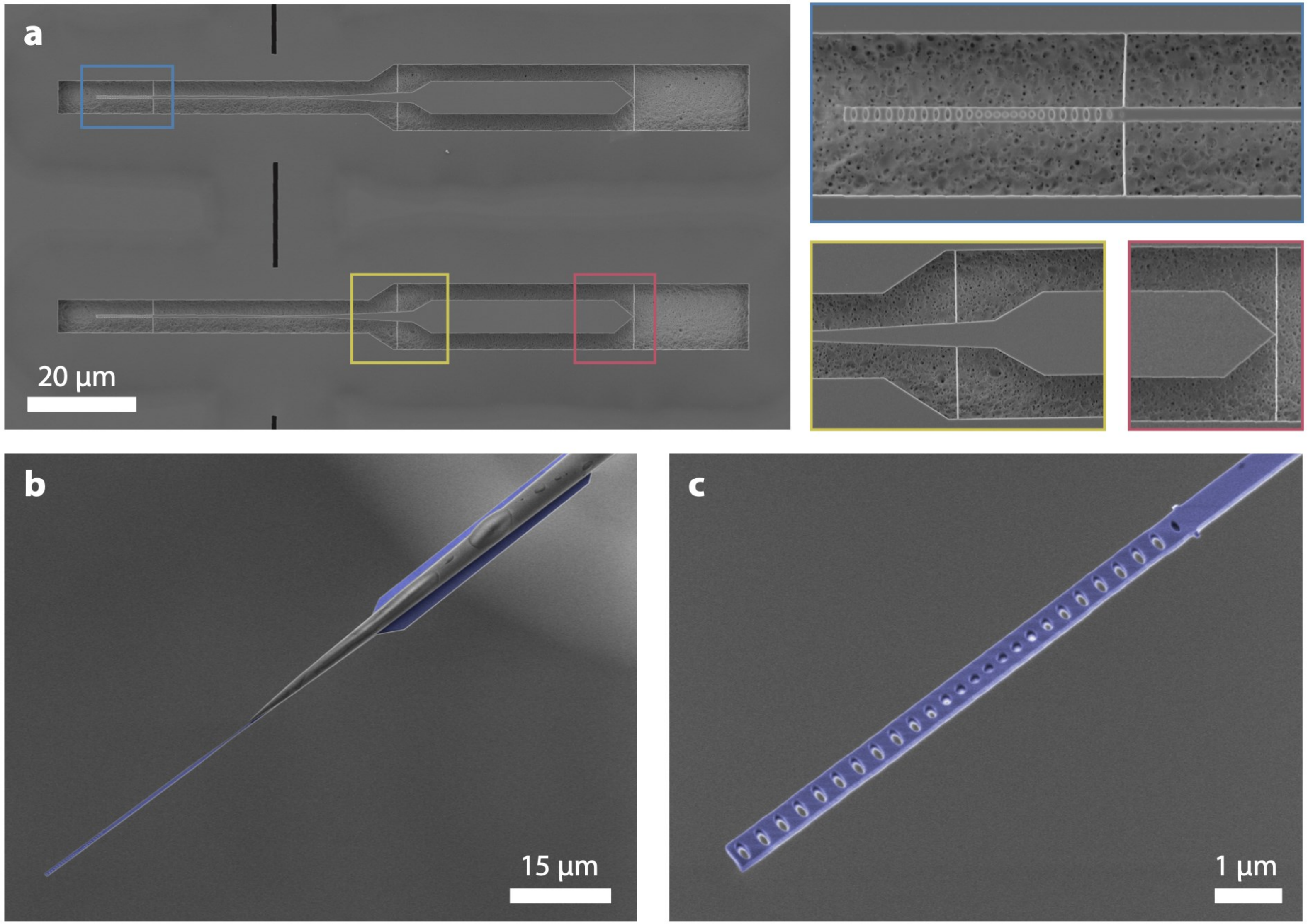

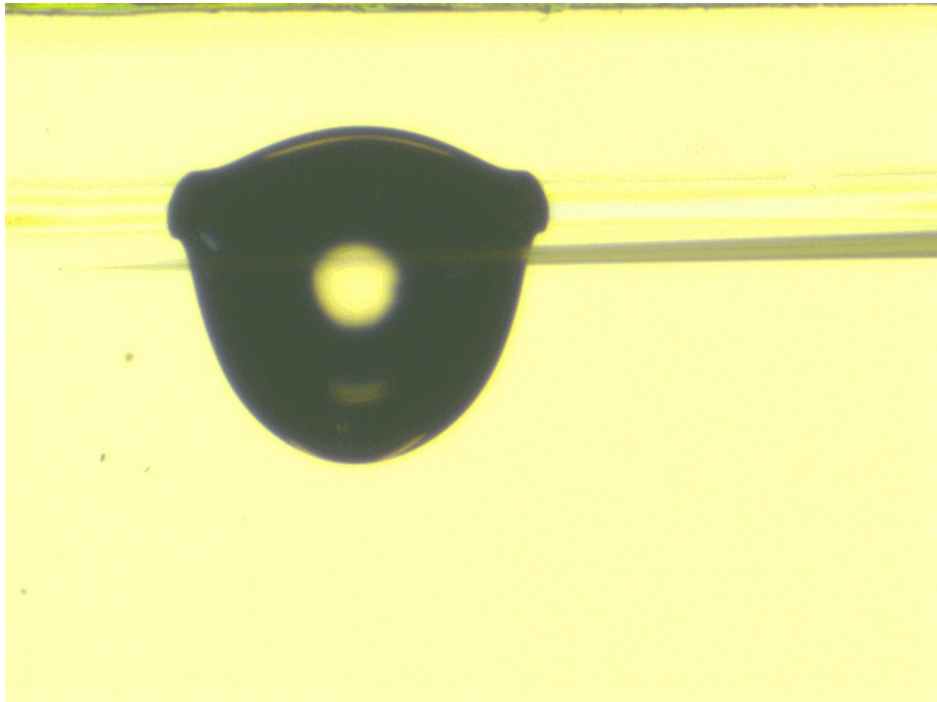

W. W. Wasserman, R. A. Harrison, G. I. Harris, A. Sawadsky, Y. L. Sfendla, W. P. Bowen, and C. G. Baker, *Cryogenic and Hermetically Sealed Packaging of Photonic Chips for Optomechanics*, Optics Express, **30**, 30822 Aug (2022).

Superfluid wavetank

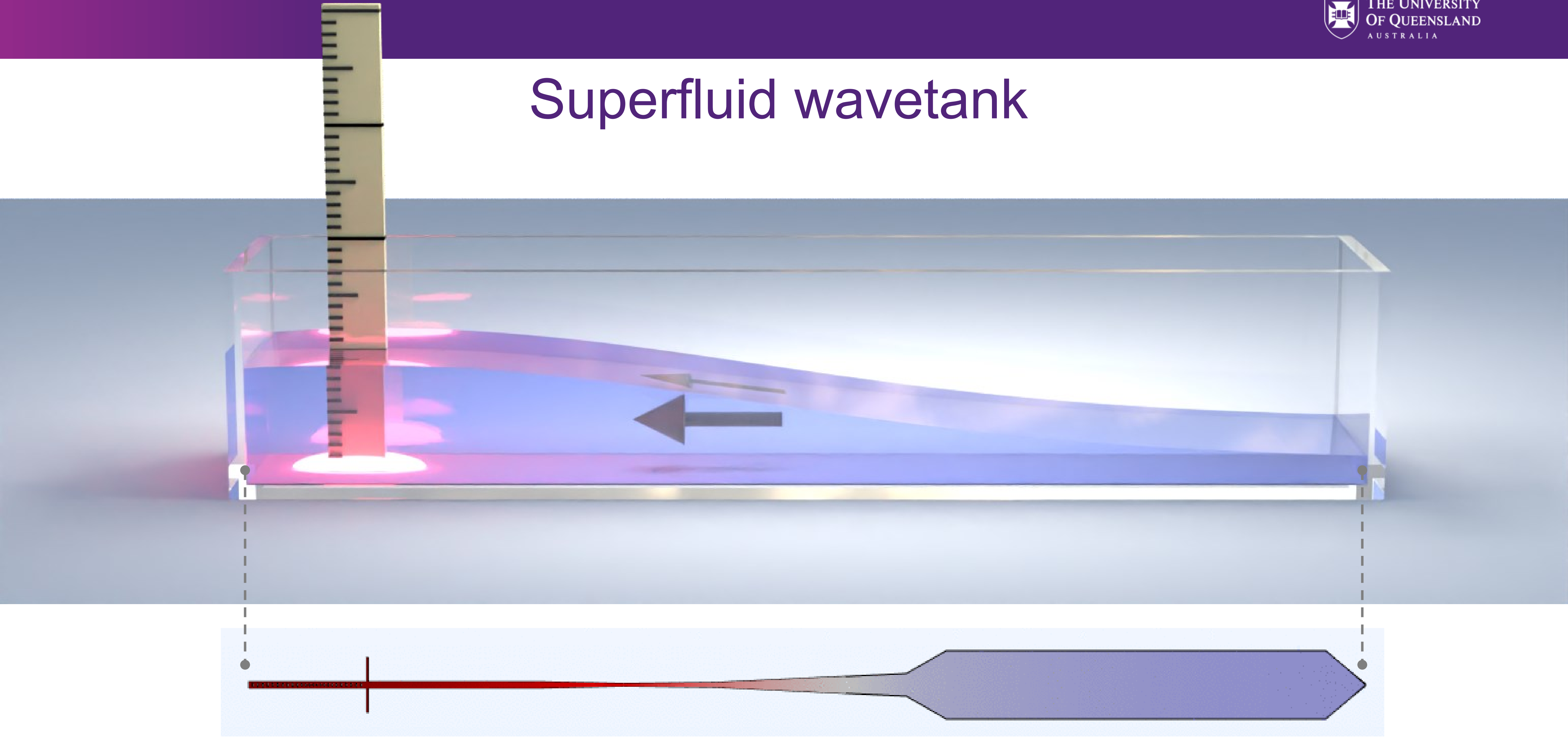

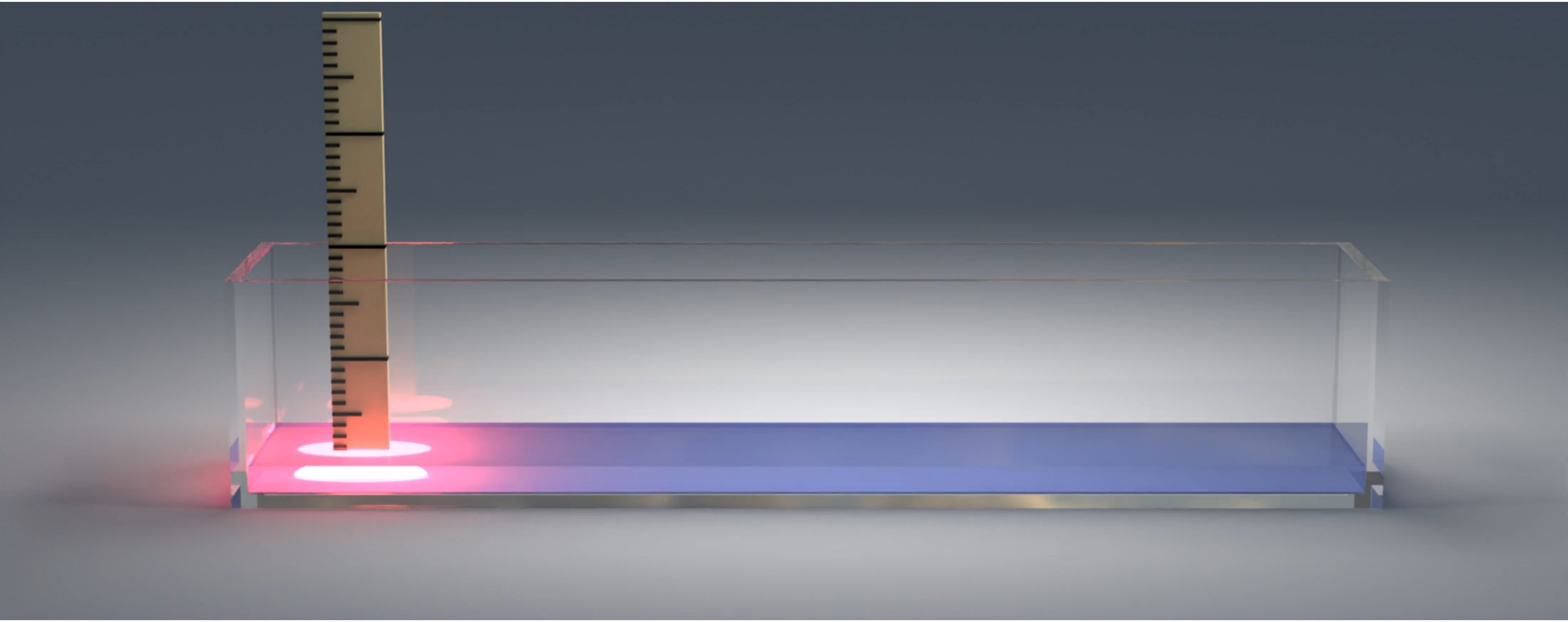

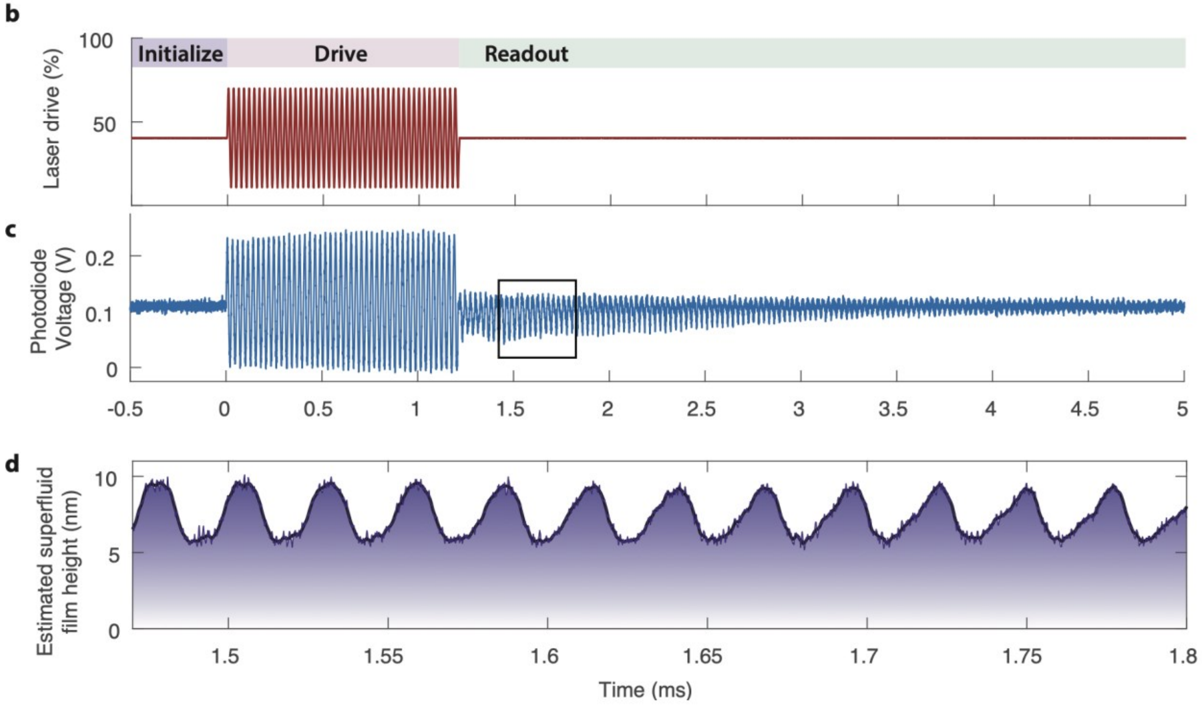
b
Initialize
Drive
Readout
Laser drive (%)
100
50
c
Photodiode Voltage (V)
0.2
0.1
0
-0.5
0
0.5
1
1.5
2
2.5
3
3.5
4
4.5
5
d
Estimated superfluid film height (nm)
10
5
0
1.5
1.55
1.6
1.65
1.7
1.75
1.8
Time (ms)

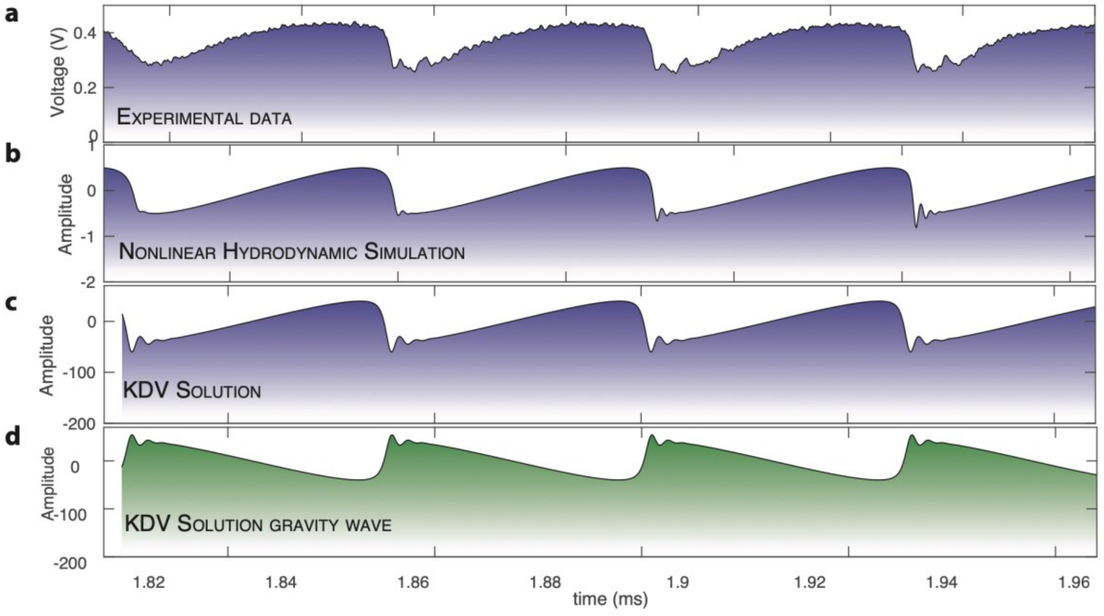
a
Voltage (V)
0.4
0.2
0
Experimental data
b
Amplitude
1
0
-1
-2
Nonlinear Hydrodynamic Simulation
c
Amplitude
0
-100
-200
KDV Solution
d
Amplitude
0
-100
-200
KDV Solution gravity wave
1.82
1.84
1.86
1.88
1.9
1.92
1.94
1.96
time (ms)

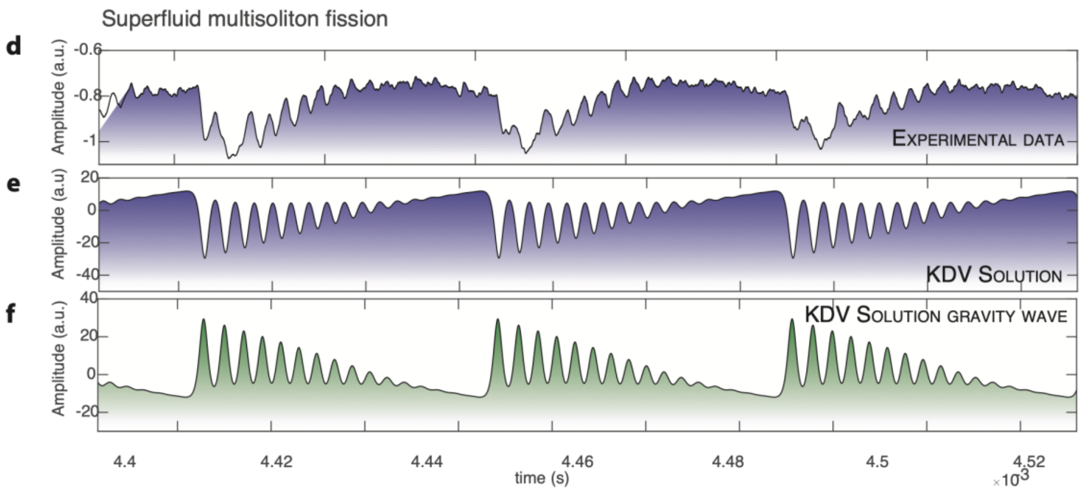
Superfluid multisoliton fission
d
Amplitude (a.u.)
-0.6
-0.8
-1
Experimental data
e
Amplitude (a.u)
20
0
-20
-40
KDV Solution
f
Amplitude (a.u.)
40
20
0
-20
KDV Solution gravity wave
4.4
4.42
4.44
4.46
4.48
4.5
4.52
time (s)
×10³

Why use cleanroom nanofabrication?

Why miniaturize?

- Scalability / cost and power reduction & integration
- Higher spatial resolution
- Higher bandwidth
- Higher sensitivity

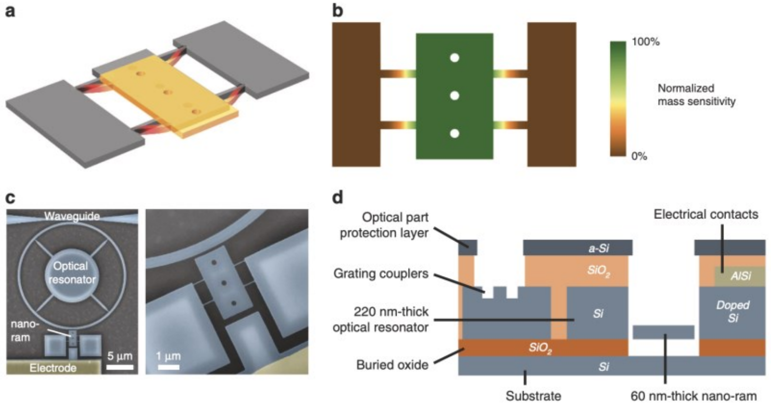

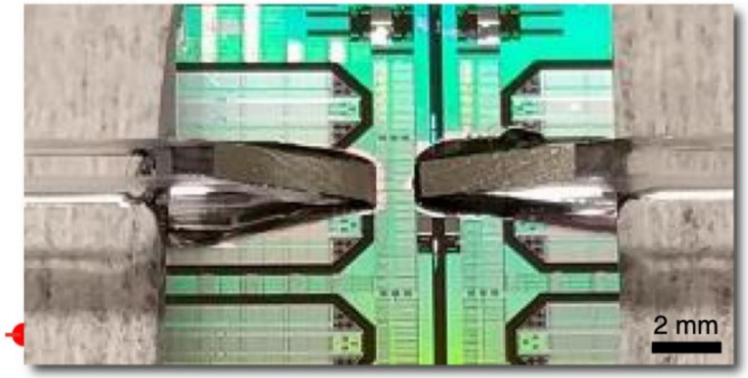

Optomechanical device with fiber transposers

Sansa, M. *et al.* Optomechanical mass spectrometry. *Nature Communications* **11**, 3781 (2020).

Biological/particle sensing using optical resonators

Frequency shift approach

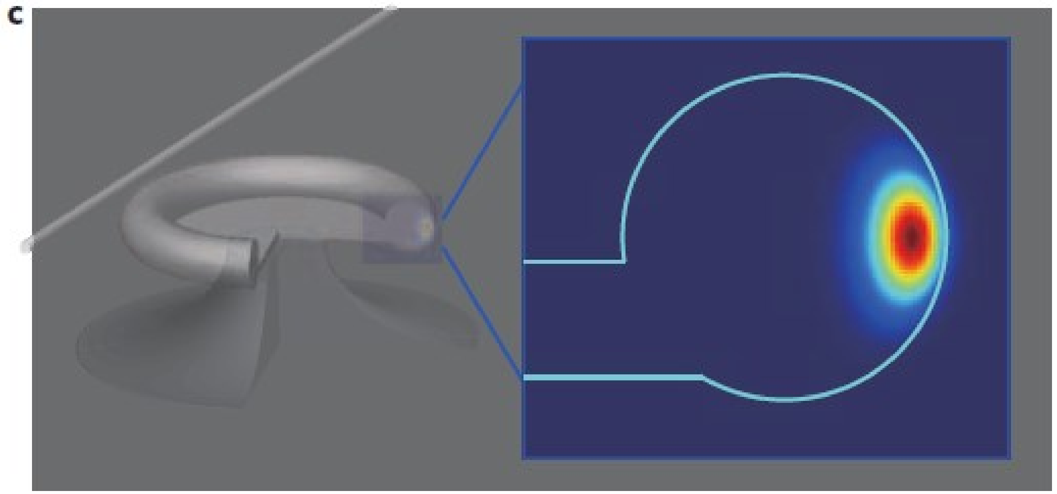

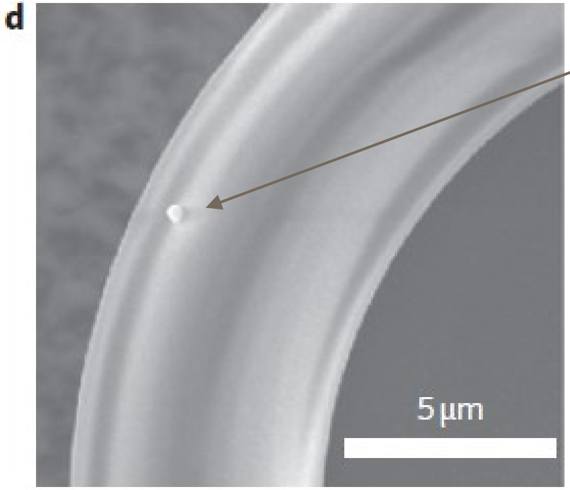

Particle lands on resonator
→ Change in effective size
→ Dispersive shift
(fundamentally analogous to cavity optomechanics !)

$$\frac{\Delta\omega}{\omega_0} = -\frac{1}{2}\frac{\int_{\text{particle}}(\varepsilon_r - 1)\left|\vec{E}\left(\vec{r}\right)\right|^2 \mathrm{d}^3\vec{r}}{\int_{\text{all}}\varepsilon_r\left(\vec{r}\right)\left|\vec{E}\left(\vec{r}\right)\right|^2 \mathrm{d}^3\vec{r}}$$

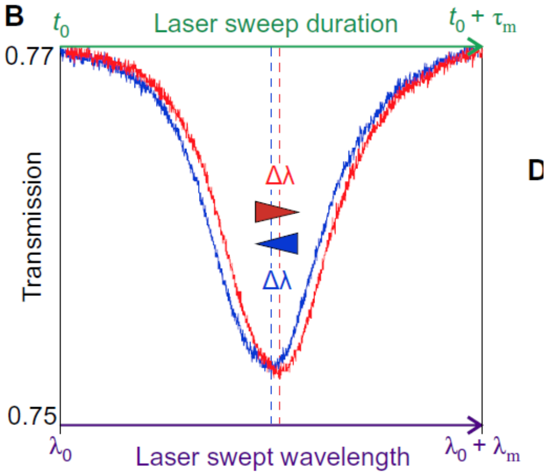

Biological/particle sensing using WGM resonators

Frequency shift approach

Answer: 1- increase optical Q. 2- Decrease mode volume → High Q/V ratio
Example: use plasmonic resonance

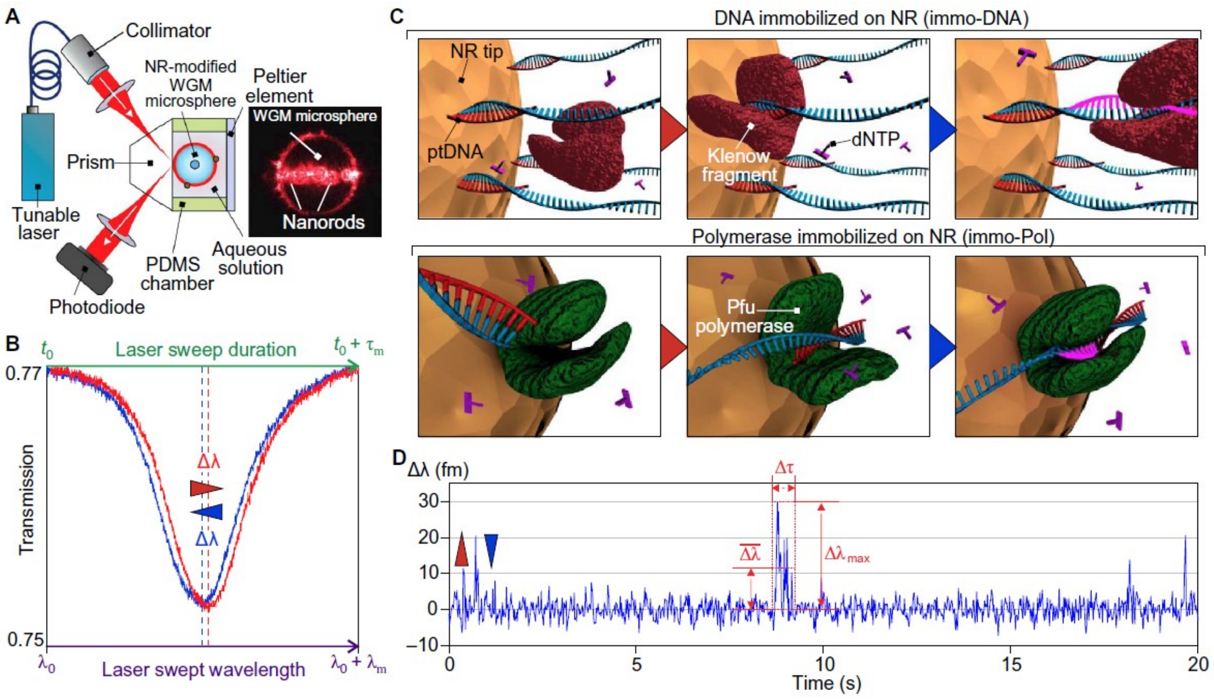

E. Kim, M. D. Baaske, I. Schuldes, P. S. Wilsch, and F. Vollmer, "Label-free optical detection of single enzyme-reactant reactions and associated conformational changes," *Science Advances*, vol. 3, no. 3, Mar. 2017.

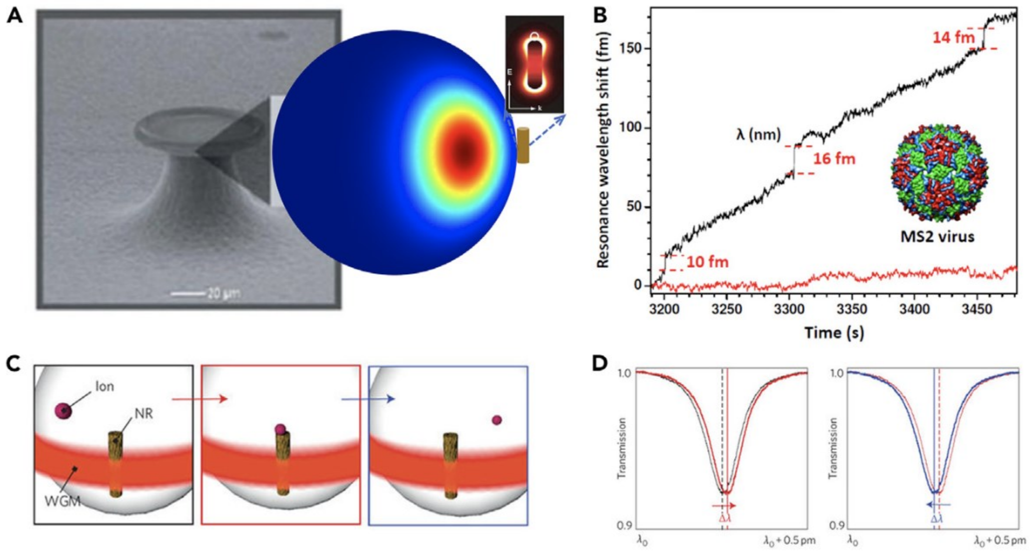

Label-Free Detection of Single Protein Using a Nanoplasmonic-Photonic Hybrid Microcavity Venkata R. Dantham et al

Small mode volume dielectric cavities

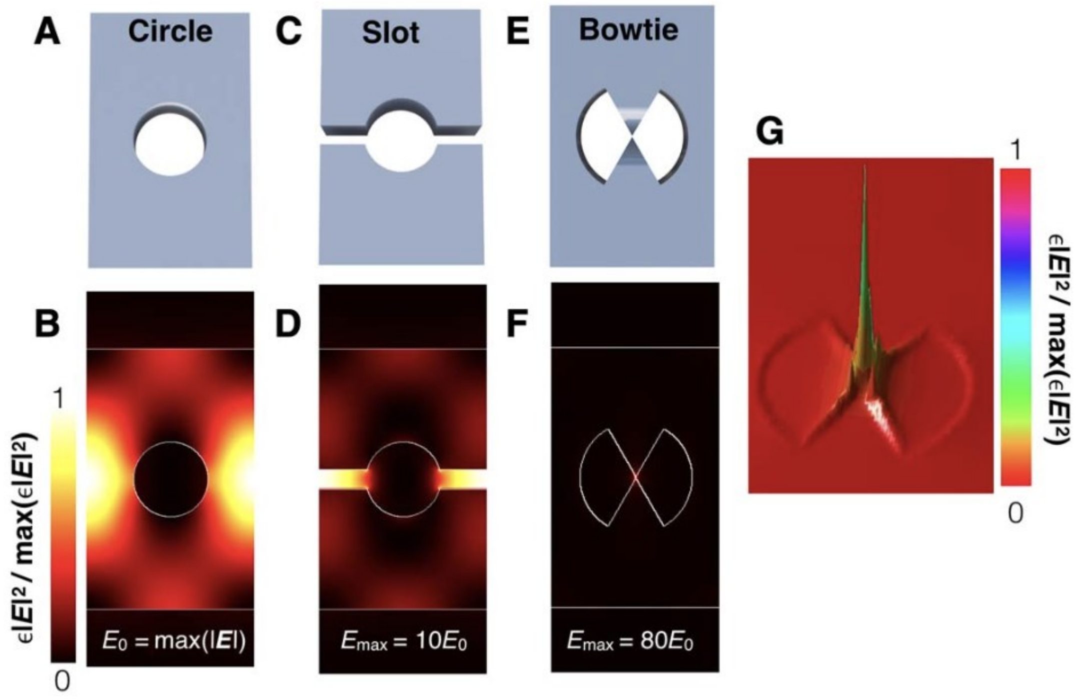

Fig. 1. Comparison of light concentration in different photonic crystal unit cells.

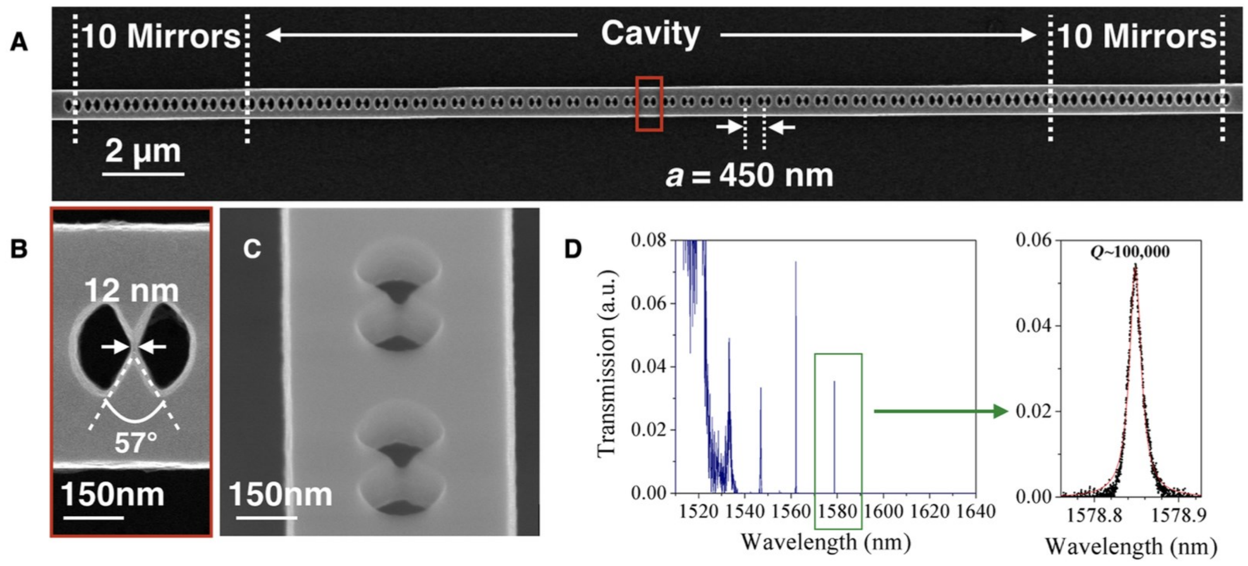

Hu, S. *et al.* Experimental realization of deep-subwavelength confinement in dielectric optical resonators. *Science Advances* **4**, eaat2355 (2018).

Choice of optical polarization

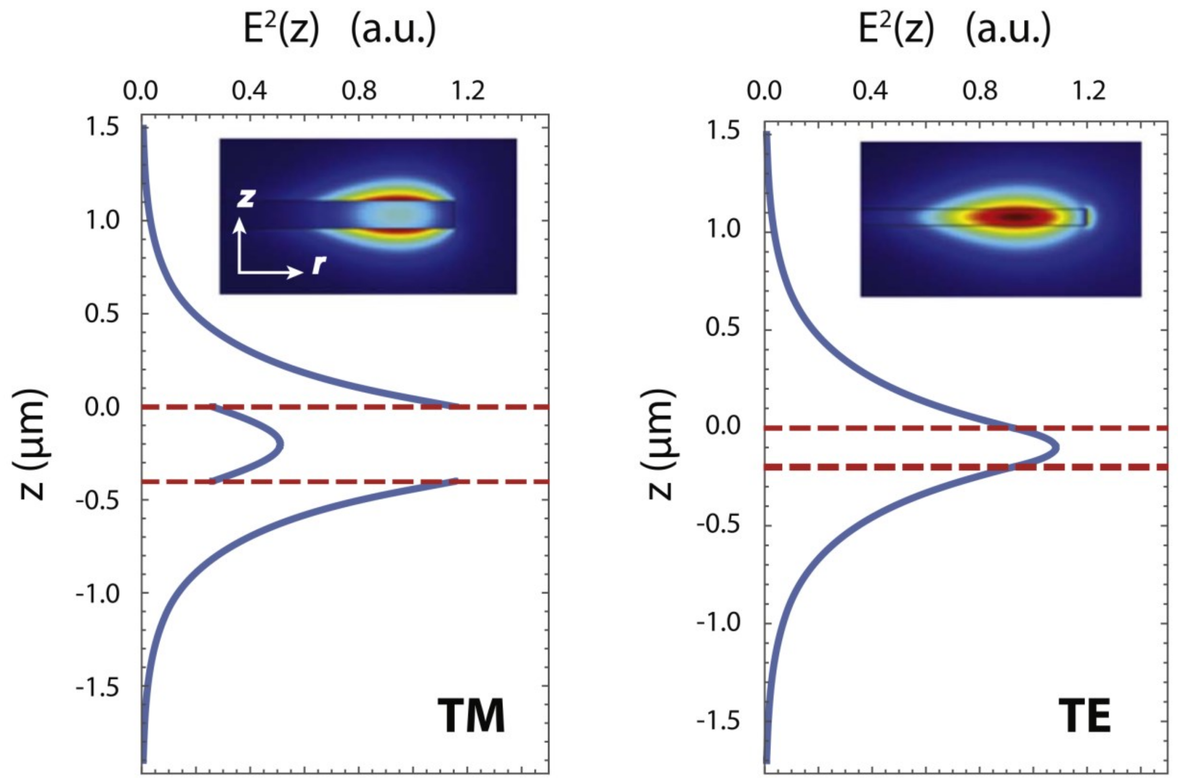

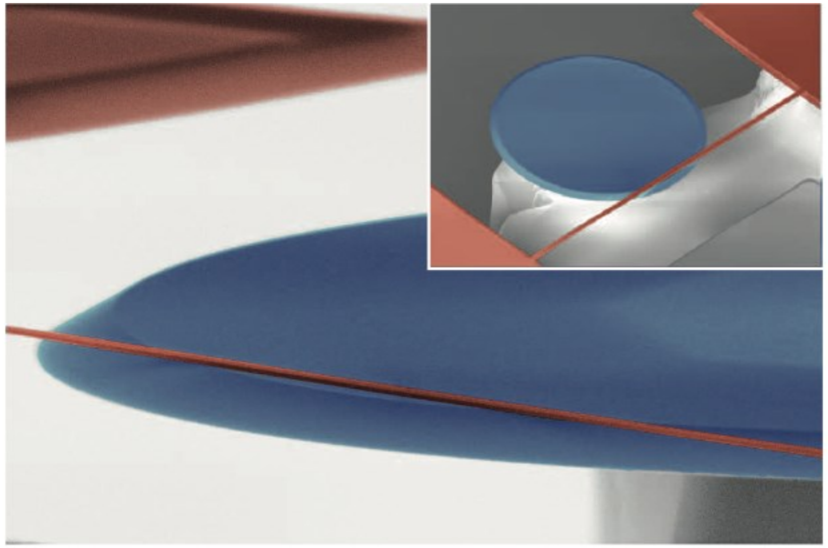

Baker, C. G. *et al. New J. Phys.* **18**, 123025 (2016).

Maximizing modal overlap

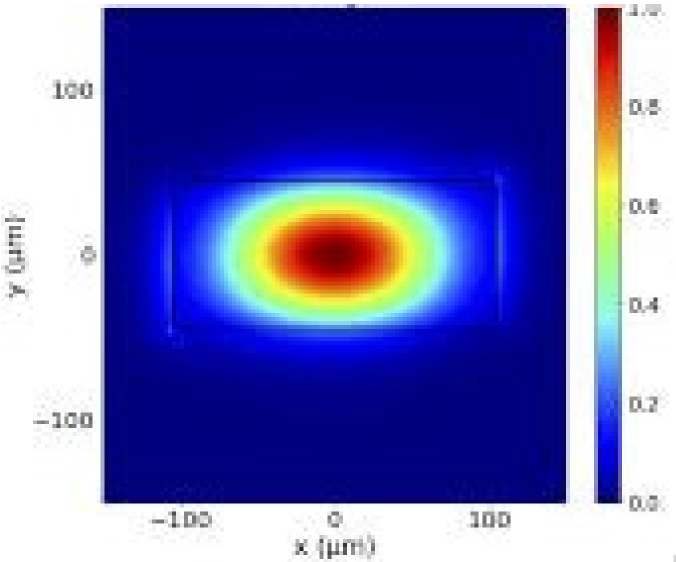

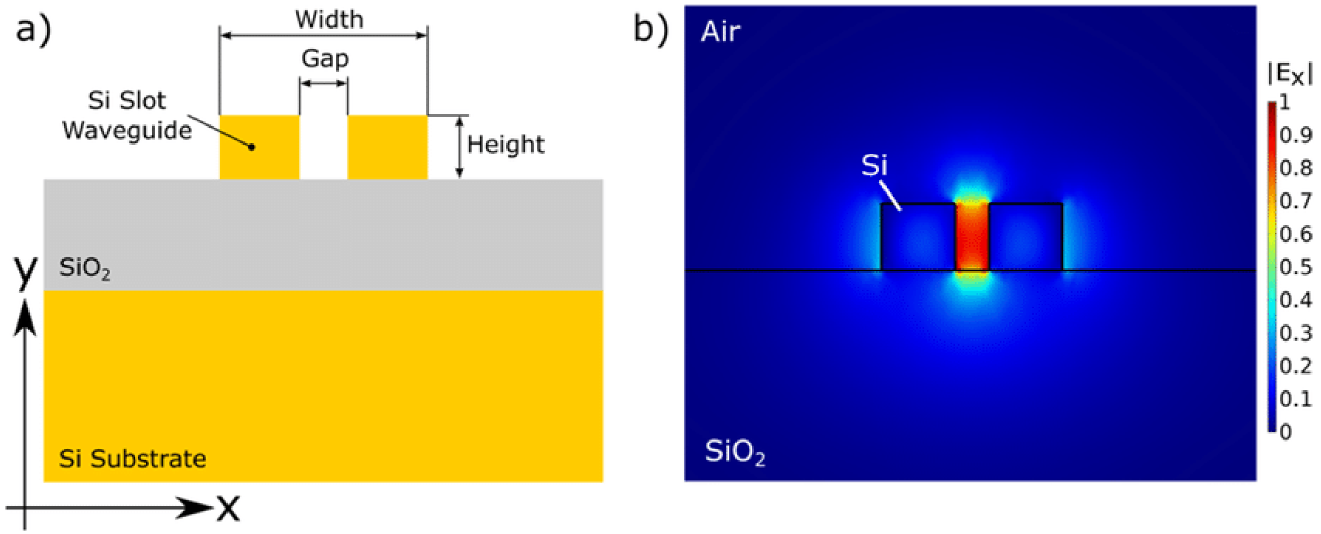

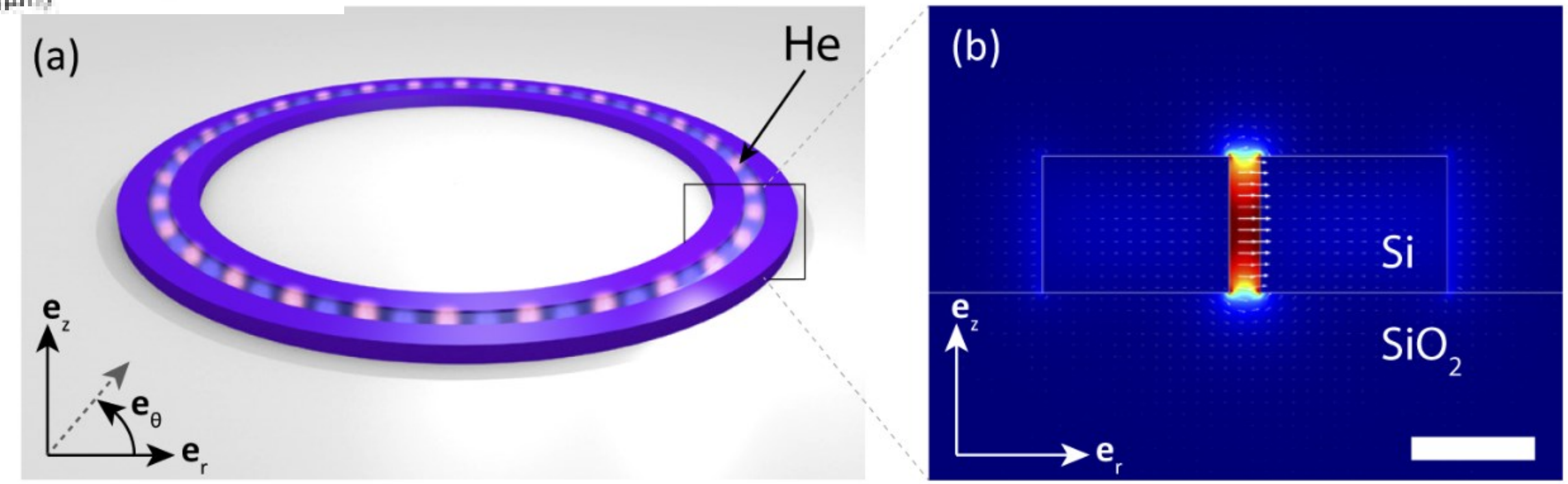

Almeida, V. R., Xu, Q., Barrios, C. A. & Lipson, M. Guiding and confining light in void nanostructure. *Opt. Lett., OL* **29**, 1209–1211 (2004).
Harris, G. I. *et al.* Proposal for a quantum traveling Brillouin resonator. *Opt. Express, OE* **28**, 22450–22461 (2020).

Review articles

- B.-B. Li, L. Ou, Y. Lei, and Y.-C. Liu, *Cavity Optomechanical Sensing*, Nanophotonics (2021).
- Ward, J. & Benson, O. WGM microresonators: sensing, lasing and fundamental optics with microspheres. *Laser & Photonics Reviews* **5**, 553–570 (2011).
- Jiang, X., Qavi, A. J., Huang, S. H. & Yang, L. Whispering-Gallery Sensors. *Matter* **3**, 371–392 (2020).

Quantum limits to sensitivity

Standard quantum limit (SQL)

Radiation pressure of light

Radiation pressure

Kepler (1619)

Radiation pressure

Kepler (1619)

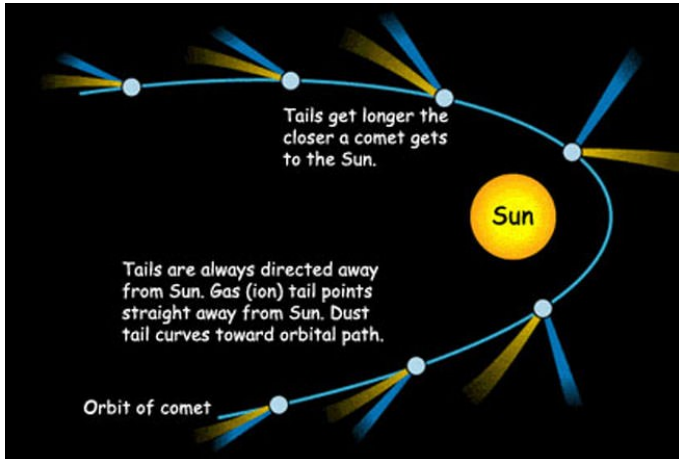

Radiation pressure

Kepler (1619)

Photons carry momentum

$$p = \frac{h}{\lambda}$$

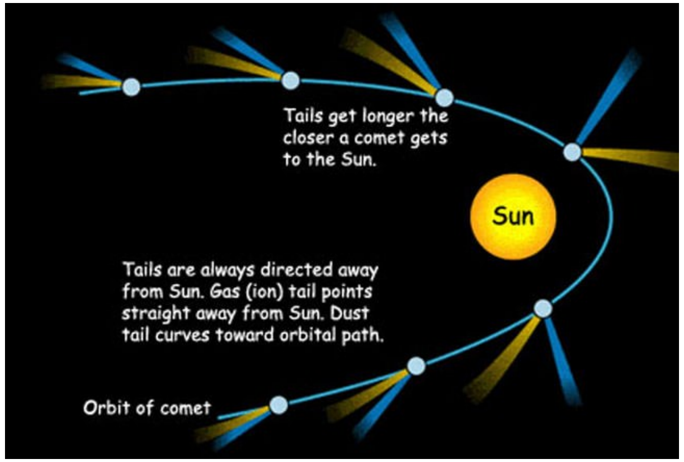

Radiation pressure

Kepler (1619)

Photons carry momentum

$$p = \frac{h}{\lambda}$$

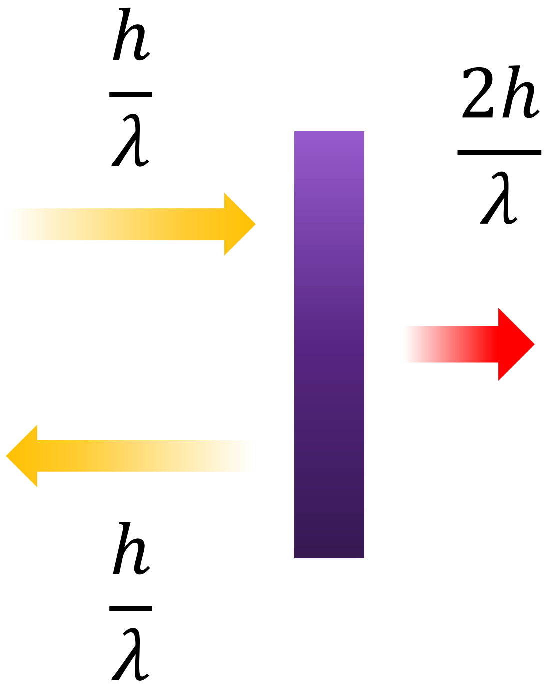

Radiation pressure

-Radiation pressure of sunlight (I=1 kW/m^2) striking the earth at normal incidence,
Case 1: Absorbed
Case 2: Reflected

$$F_{rad} = \frac{dp}{dt} = \frac{I}{h\nu} \times \frac{h}{\lambda} = \frac{I}{c}$$
$$= \sim \frac{10^3}{3 \cdot 10^8} \sim 3\ \mu N$$

$$p = \frac{h}{\lambda}$$

$$E = h\nu$$

$$P_{rad,abs} = 3\ \mu\text{Pa}$$

$$P_{rad,reflection} = 6\ \mu\text{Pa}$$

→~10^{10} times smaller than atmospheric pressure

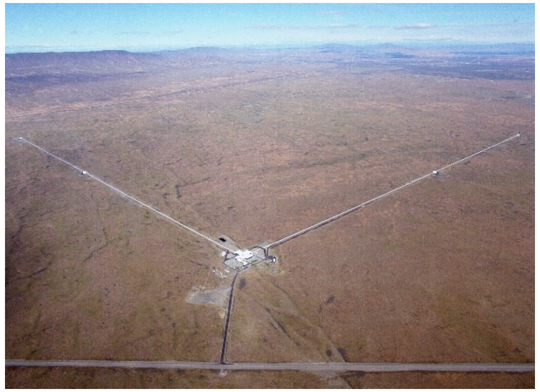

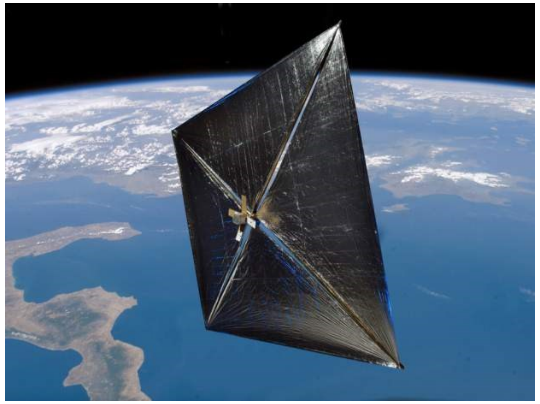

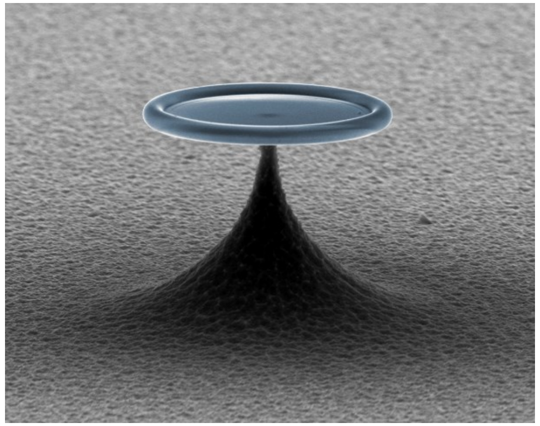

Experimental detection of radiation pressure

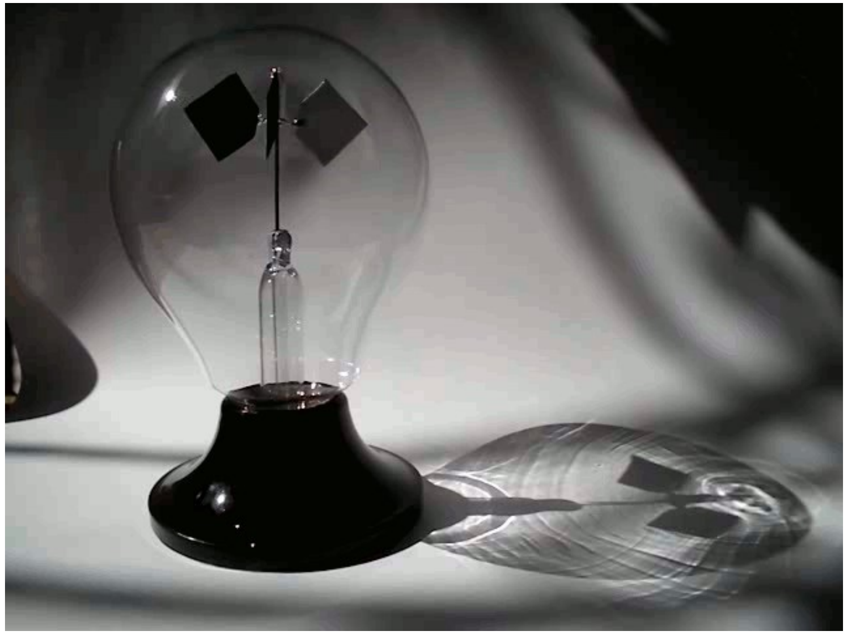

Crookes radiometer (1873)

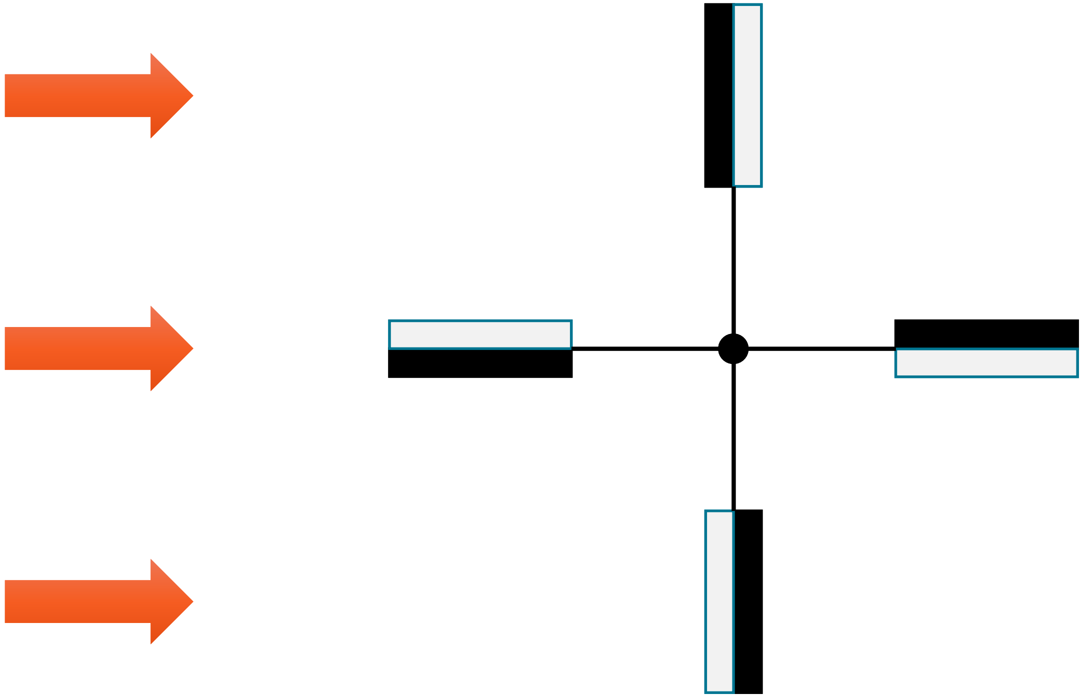

Experimental detection of radiation pressure

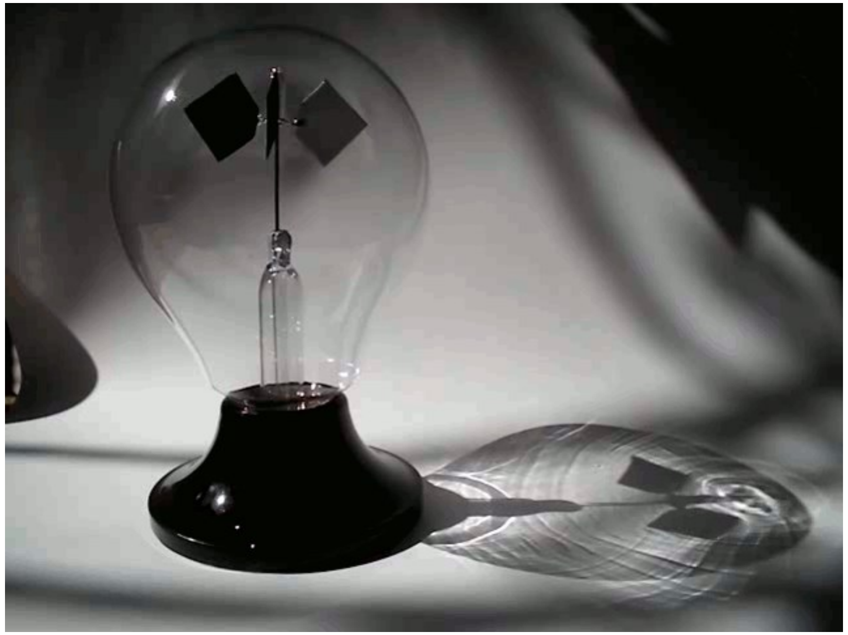

Crookes radiometer (1873)

Which direction do the blades spin in ?

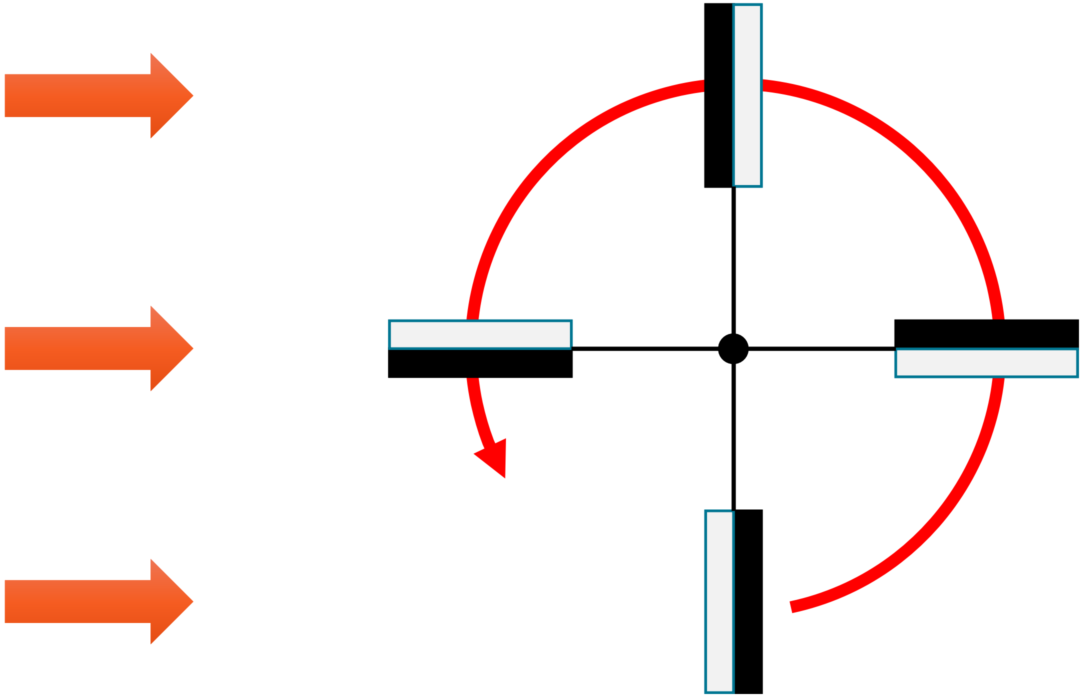

Experimental detection of radiation pressure

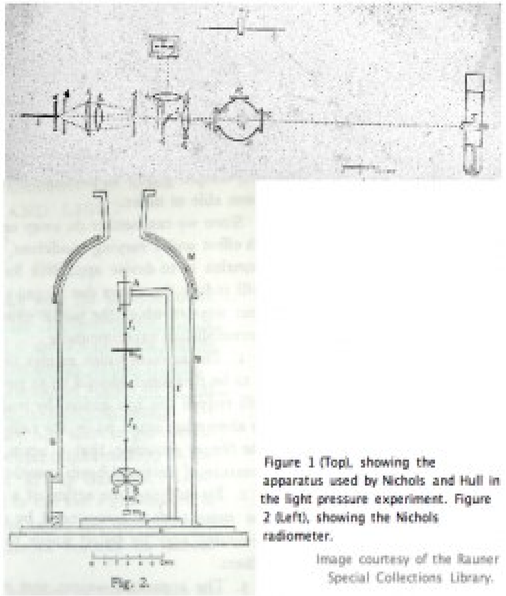

Figure 1 (Top), showing the apparatus used by Nichols and Hull in the light pressure experiment. Figure 2 (Left), showing the Nichols radiometer.

Image courtesy of the Rauner Special Collections Library.

Experimental detection
Nichols and Hull, 1901

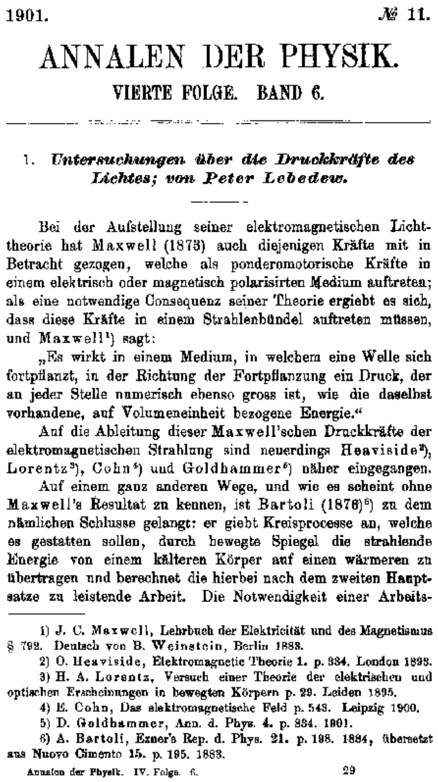

1901. № 11.

ANNALEN DER PHYSIK.

VIERTE FOLGE. BAND 6.

1. *Untersuchungen über die Druckkräfte des Lichtes; von Peter Lebedew.*

Bei der Aufstellung seiner elektromagnetischen Lichttheorie hat Maxwell (1873) auch diejenigen Kräfte mit in Betracht gezogen, welche als ponderomotorische Kräfte in einem elektrisch oder magnetisch polarisirten Medium auftreten; als eine notwendige Consequenz seiner Theorie ergiebt es sich, dass diese Kräfte in einem Strahlenbündel auftreten müssen, und Maxwell[1]) sagt:

„Es wirkt in einem Medium, in welchem eine Welle sich fortpflanzt, in der Richtung der Fortpflanzung ein Druck, der an jeder Stelle numerisch ebenso gross ist, wie die daselbst vorhandene, auf Volumeneinheit bezogene Energie.“

Auf die Ableitung dieser Maxwell'schen Druckkräfte der elektromagnetischen Strahlung sind neuerdings Heaviside[2]), Lorentz[3]), Cohn[4]) und Goldhammer[5]) näher eingegangen.

Auf einem ganz anderen Wege, und wie es scheint ohne Maxwell's Resultat zu kennen, ist Bartoli (1876)[6]) zu dem nämlichen Schlusse gelangt: er giebt Kreisprocesse an, welche es gestatten sollen, durch bewegte Spiegel die strahlende Energie von einem kälteren Körper auf einen wärmeren zu übertragen und berechnet die hierbei nach dem zweiten Hauptsatze zu leistende Arbeit. Die Notwendigkeit einer Arbeits-

1) J. C. Maxwell, Lehrbuch der Elektricität und des Magnetismus § 792. Deutsch von B. Weinstein, Berlin 1883.
2) O. Heaviside, Elektromagnetic Theorie 1. p. 334. London 1893.
3) H. A. Lorentz, Versuch einer Theorie der elektrischen und optischen Erscheinungen in bewegten Körpern p. 29. Leiden 1895.
4) E. Cohn, Das elektromagnetische Feld p. 543. Leipzig 1900.
5) D. Goldhammer, Ann. d. Phys. 4. p. 834. 1901.
6) A. Bartoli, Exner's Rep. d. Phys. 21. p. 198. 1884, übersetzt aus Nuovo Cimento 15. p. 195. 1883.

Annalen der Physik. IV. Folge. 6. 29

Peter Lebedev

E. F. Nichols and G. F. Hull, ‘The pressure due to radiation," Proceedings of the American Academy of Arts and Sciences, vol. 38, no. 20, pp. 559-599, 1903.

Lebedew, P. (1901). "Untersuchungen über die Druckkräfte des Lichtes". Annalen der Physik. ***311*** *(11): 433–458*

Standard quantum limit

Standard quantum limit (SQL)

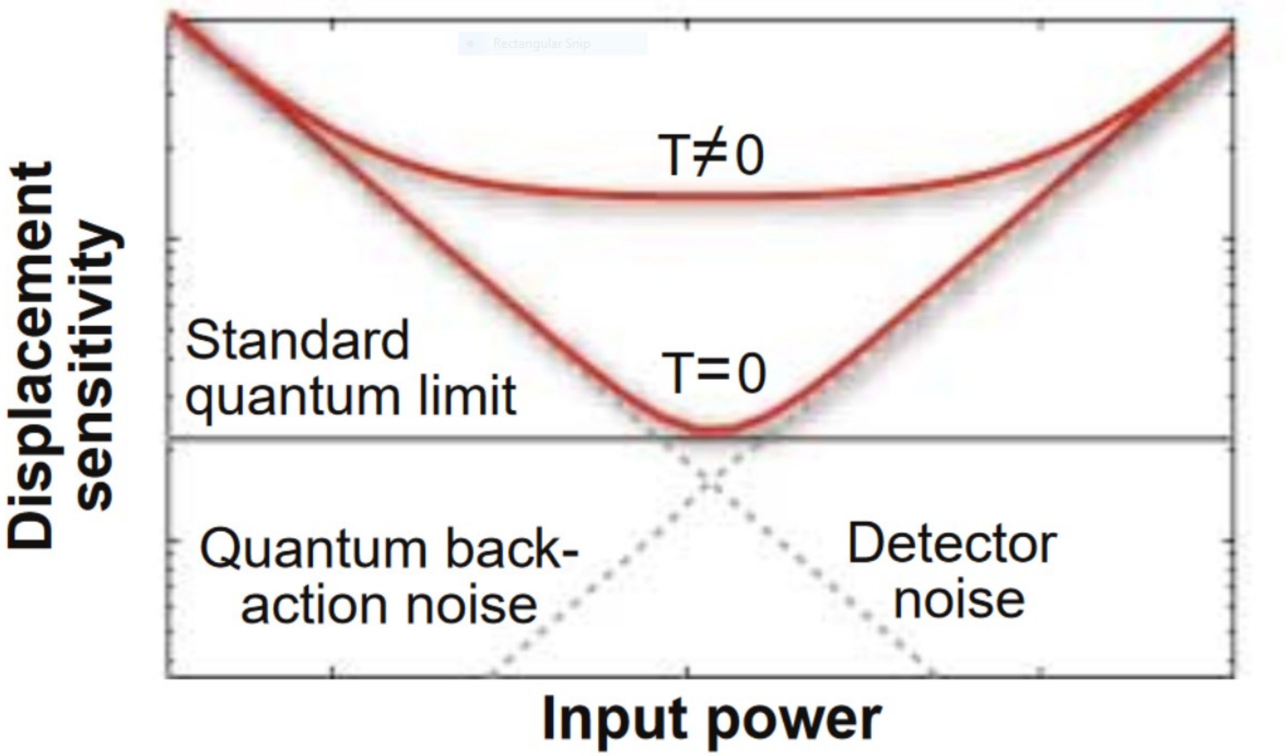

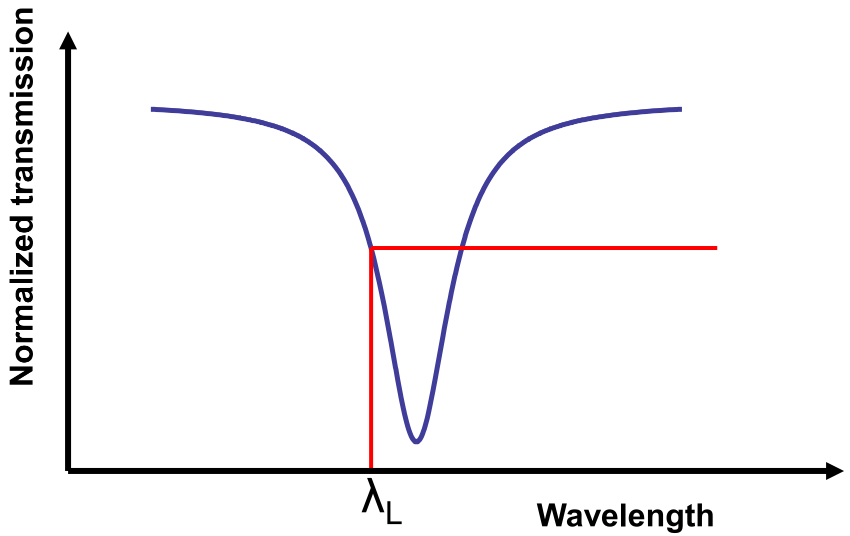

Measured photodetector intensity
→ resonator position

T. J. Kippenberg and K. J. Vahala, *Cavity Optomechanics: Back-Action at the Mesoscale*, Science **321**, 1172 (2008).

Standard quantum limit (SQL)

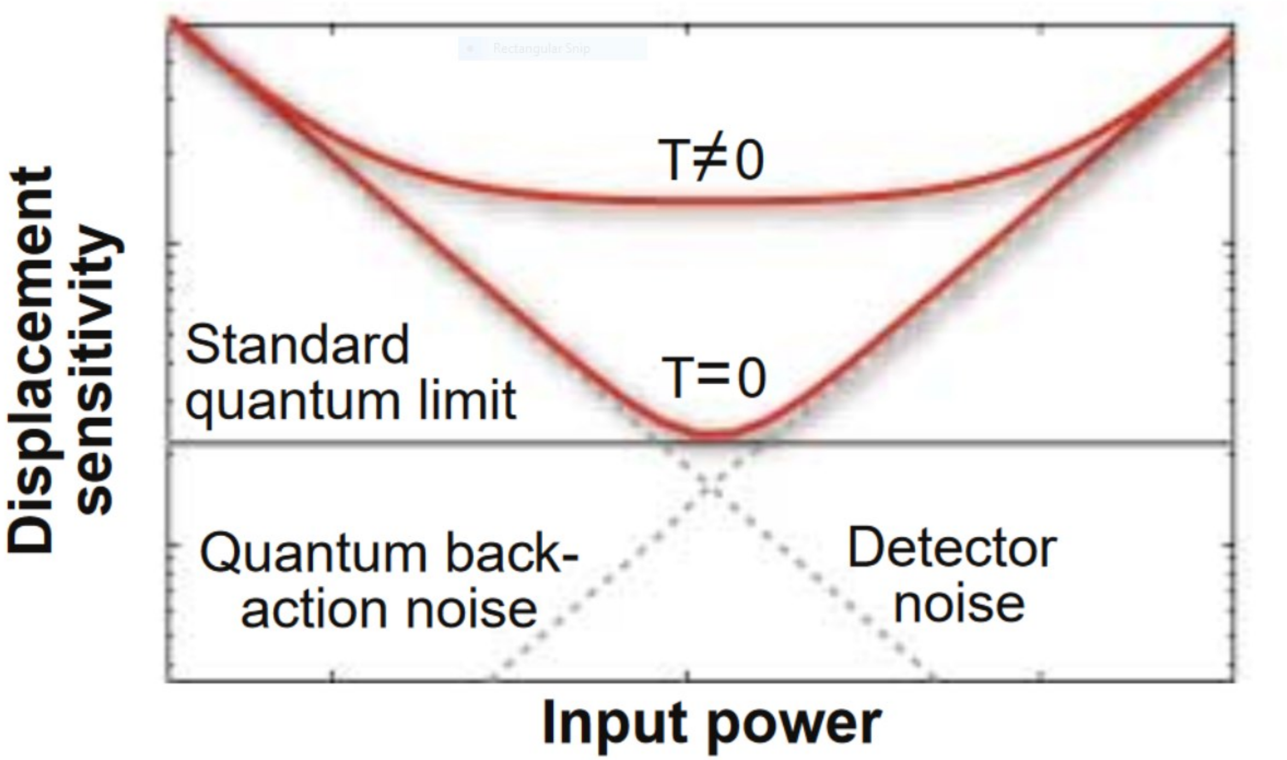

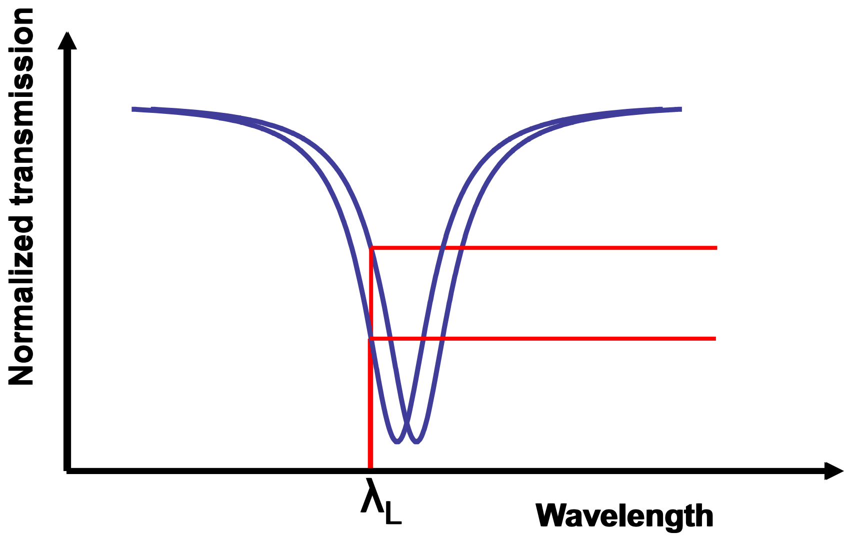

Measured photodetector intensity
→ resonator position

Influence of shot noise

T. J. Kippenberg and K. J. Vahala, *Cavity Optomechanics: Back-Action at the Mesoscale*, Science **321**, 1172 (2008).

Fluctuation of photons on photodetector results in fluctuating power measurement

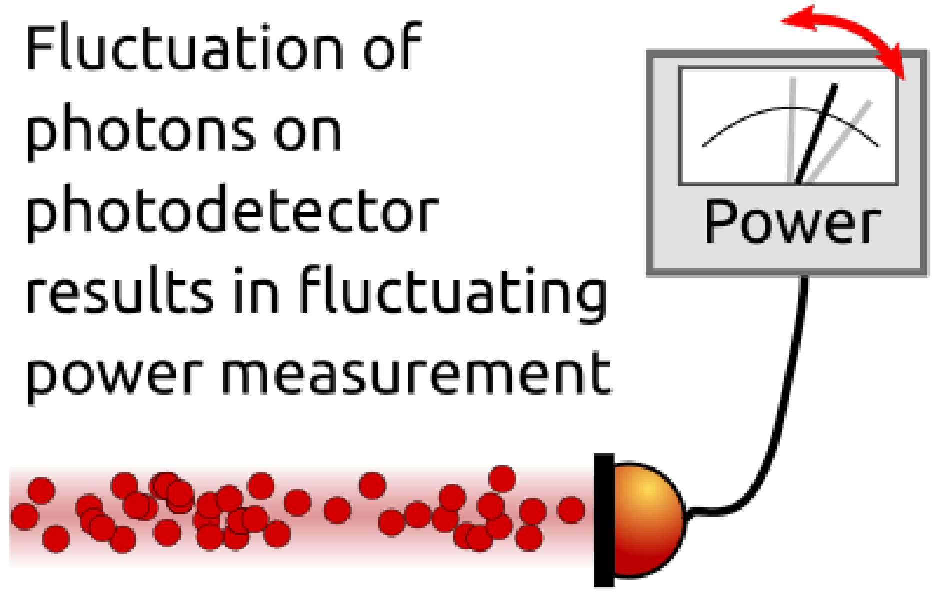

$$\Phi = \frac{10^{-9}}{2.0 \times (1.6 \times 10^{-19})} = 3.1 \times 10^{9} \text{ photons s}^{-1}.$$

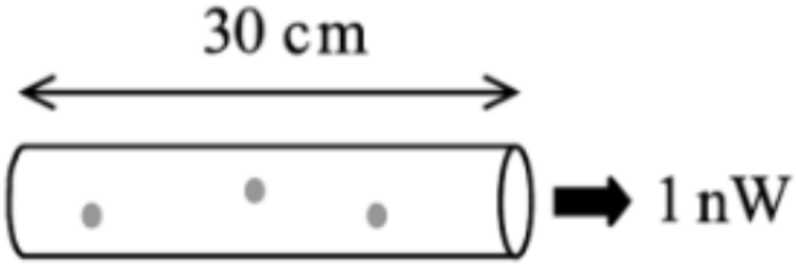

https://10m.aei.mpg.de/standard-quantum-limit-sql/
https://www.kth.se/social/files/5e8685f338d153ef15d4ee30/lecture-2-photon-statistics.pdf

Standard quantum limit (SQL)

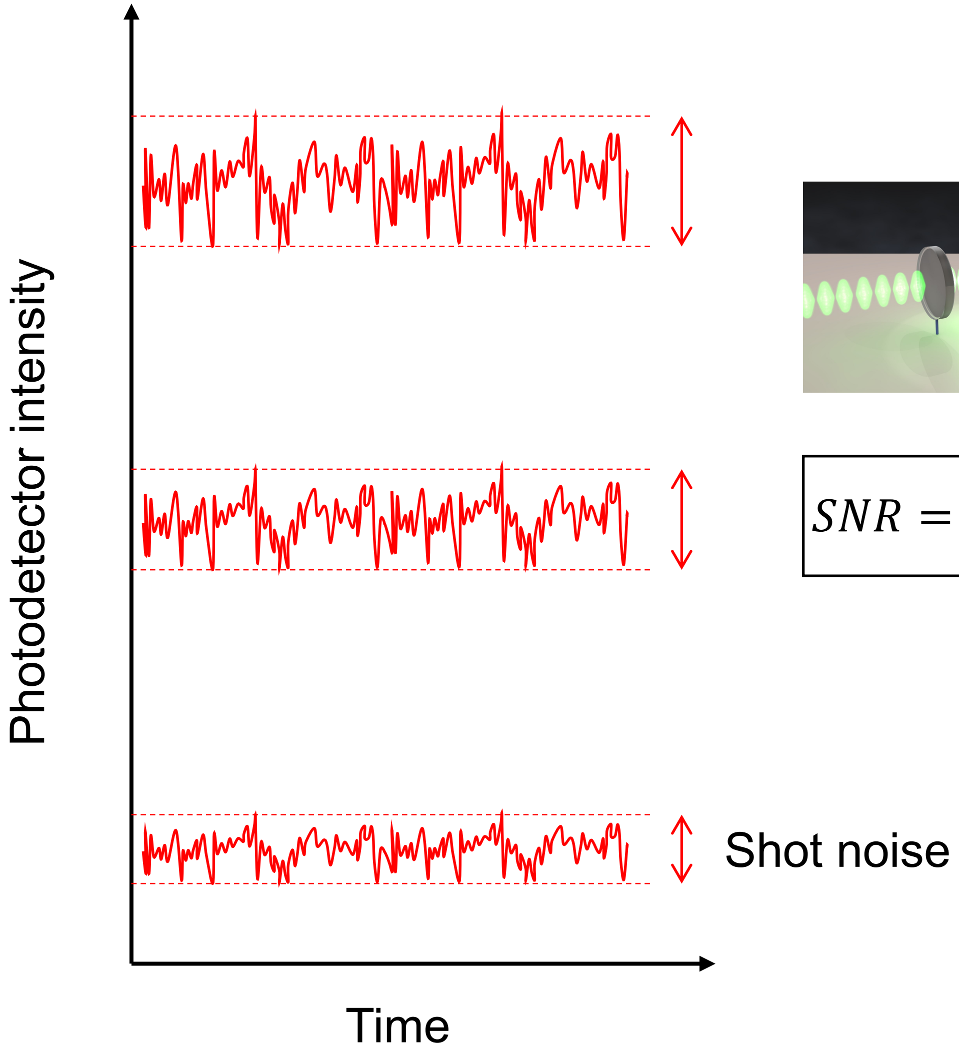

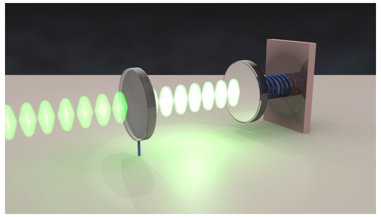

$$SNR = \frac{N}{\sqrt{N}} = \sqrt{N}$$

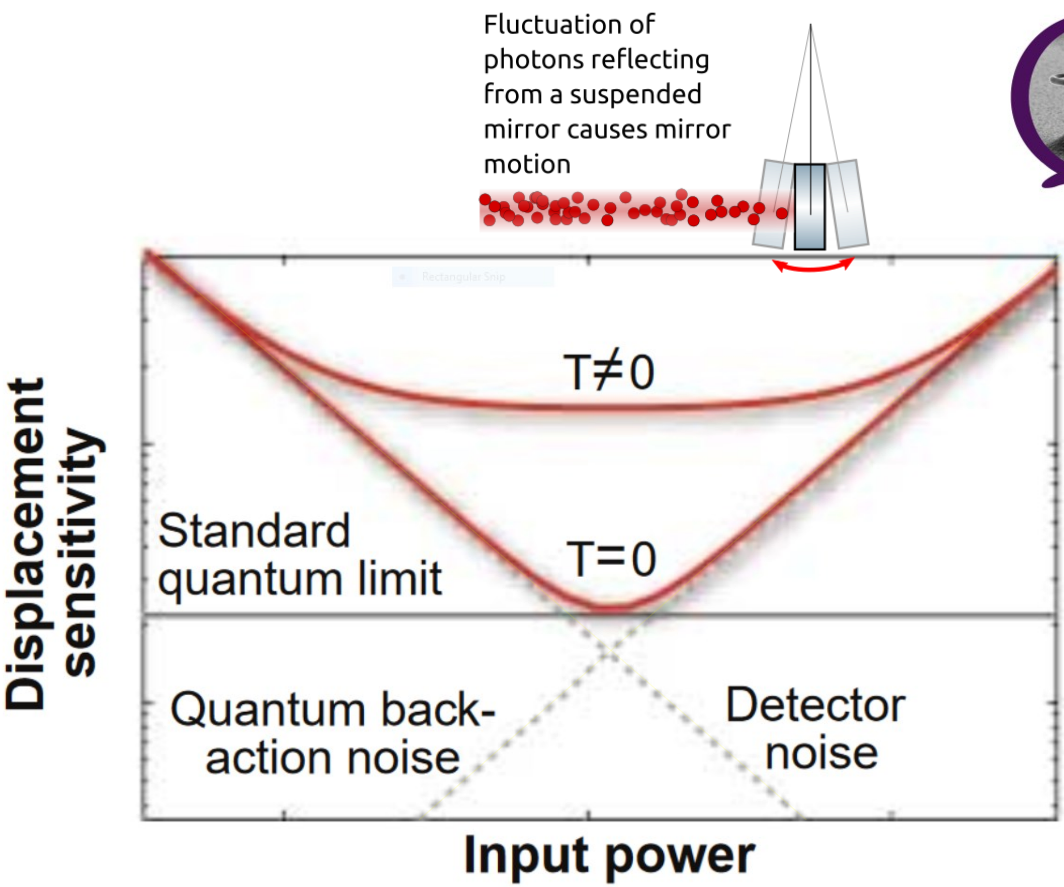

Photons imparts a random kicks, effect on momentum and position grow as $\sqrt{N}$ = 'backaction noise'

→ At the SQL, detector noise and quantum back-action noise contribute each a position uncertainty equal to half of the zero-point motion.

Observation of back-action noise

Observation of Radiation Pressure Shot Noise on a Macroscopic Object

T. P. Purdy,[1,2]* R. W. Peterson,[1,2] C. A. Regal[1,2]

The quantum mechanics of position measurement of a macroscopic object is typically inaccessible because of strong coupling to the environment and classical noise. In this work, we monitor a mechanical resonator subject to an increasingly strong continuous position measurement and observe a quantum mechanical back-action force that rises in accordance with the Heisenberg uncertainty limit. For our optically based position measurements, the back-action takes the form of a fluctuating radiation pressure from the Poisson-distributed photons in the coherent measurement field, termed radiation pressure shot noise. We demonstrate a back-action force that is comparable in magnitude to the thermal forces in our system. Additionally, we observe a temporal correlation between fluctuations in the radiation force and in the position of the resonator.

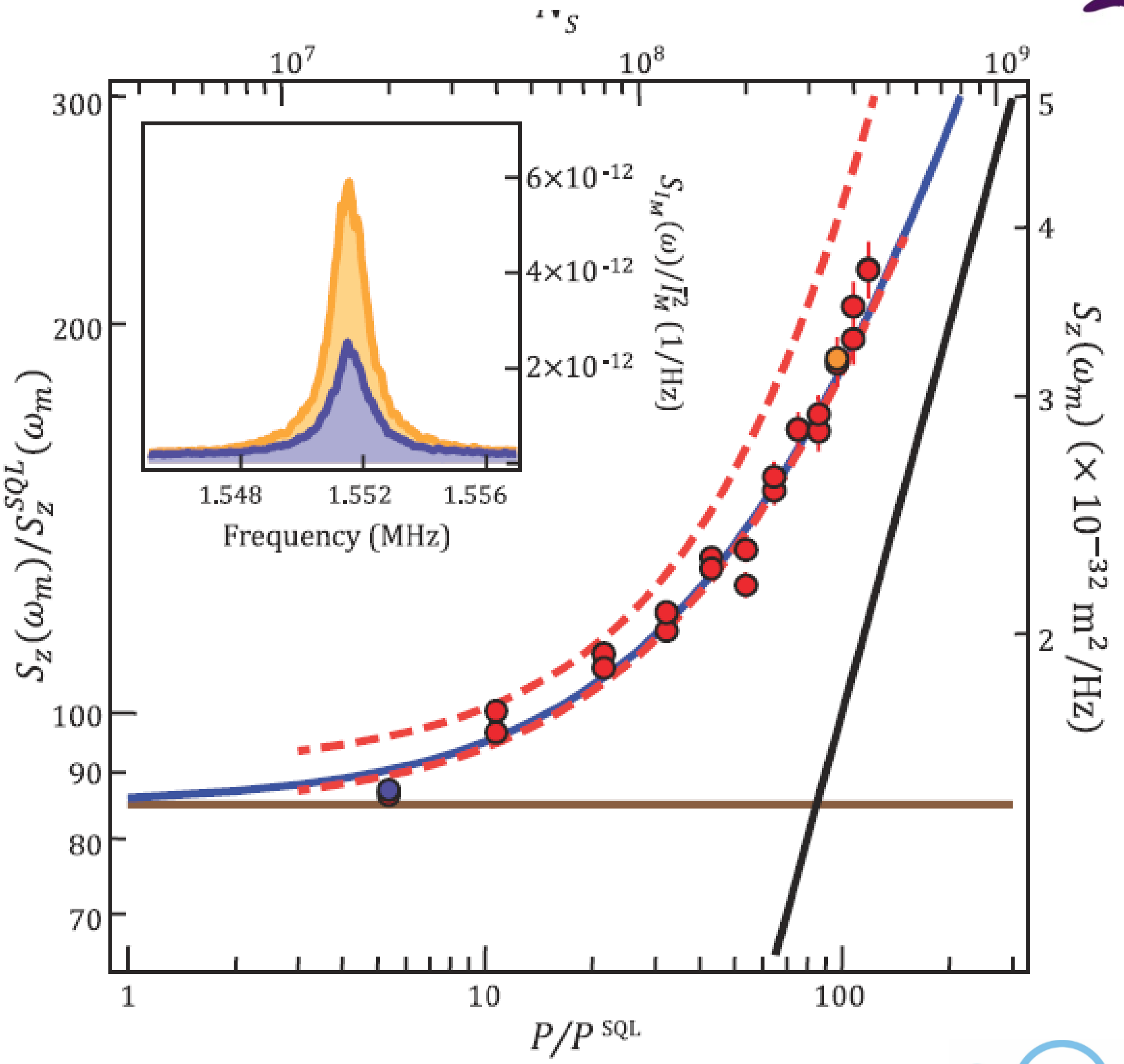

Purdy, T. P., R. W. Peterson, and C. A. Regal. "Observation of Radiation Pressure Shot Noise on a Macroscopic Object." Science 339, no. 6121 (February 15, 2013)

Photonic chip demo

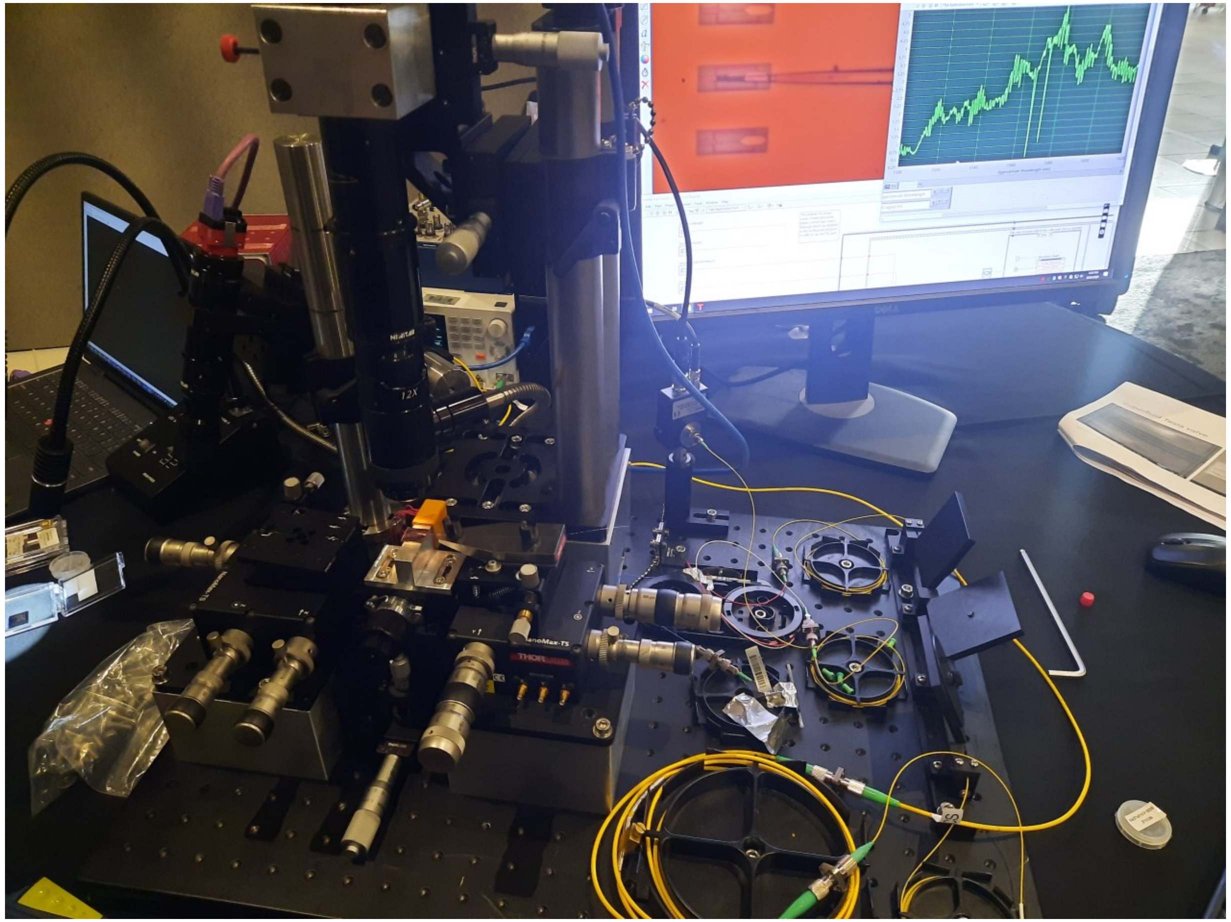

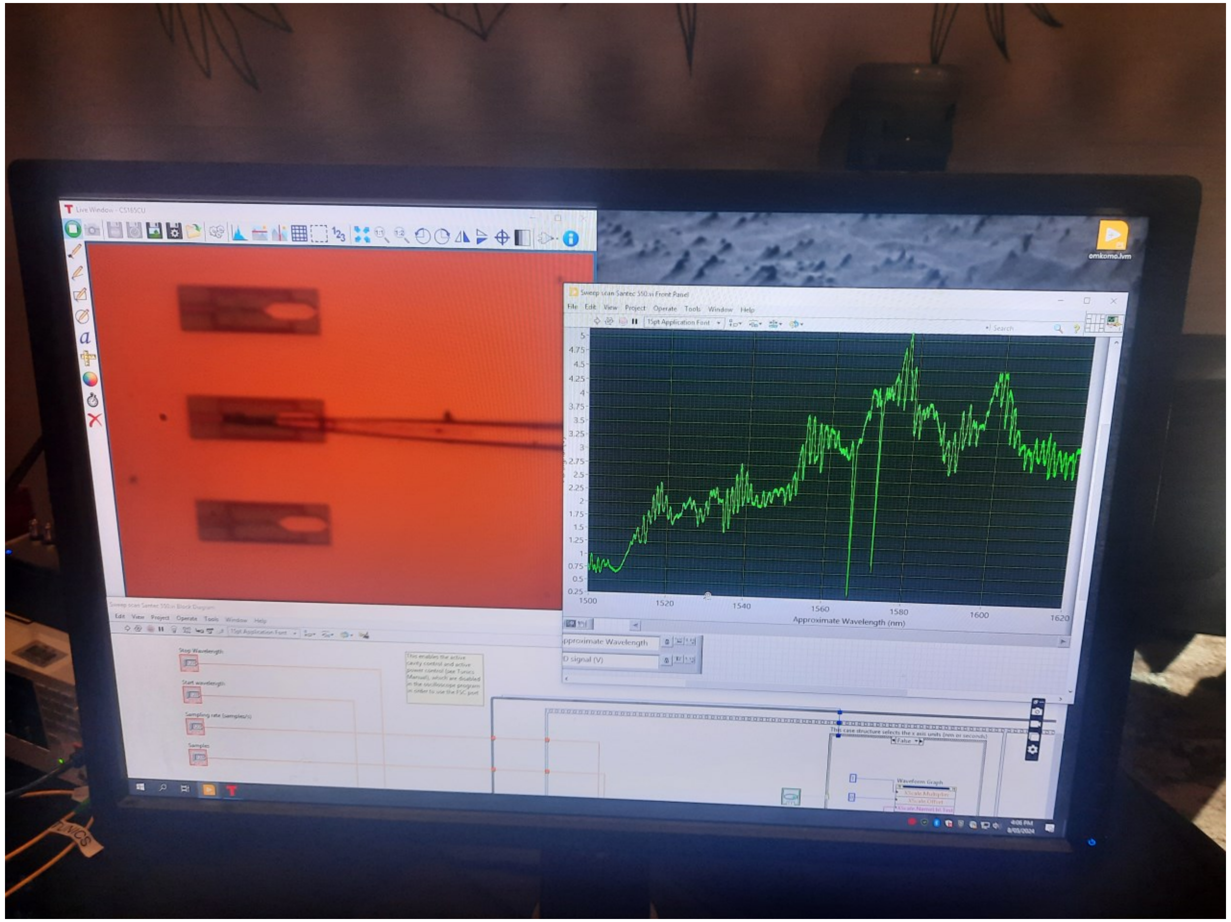

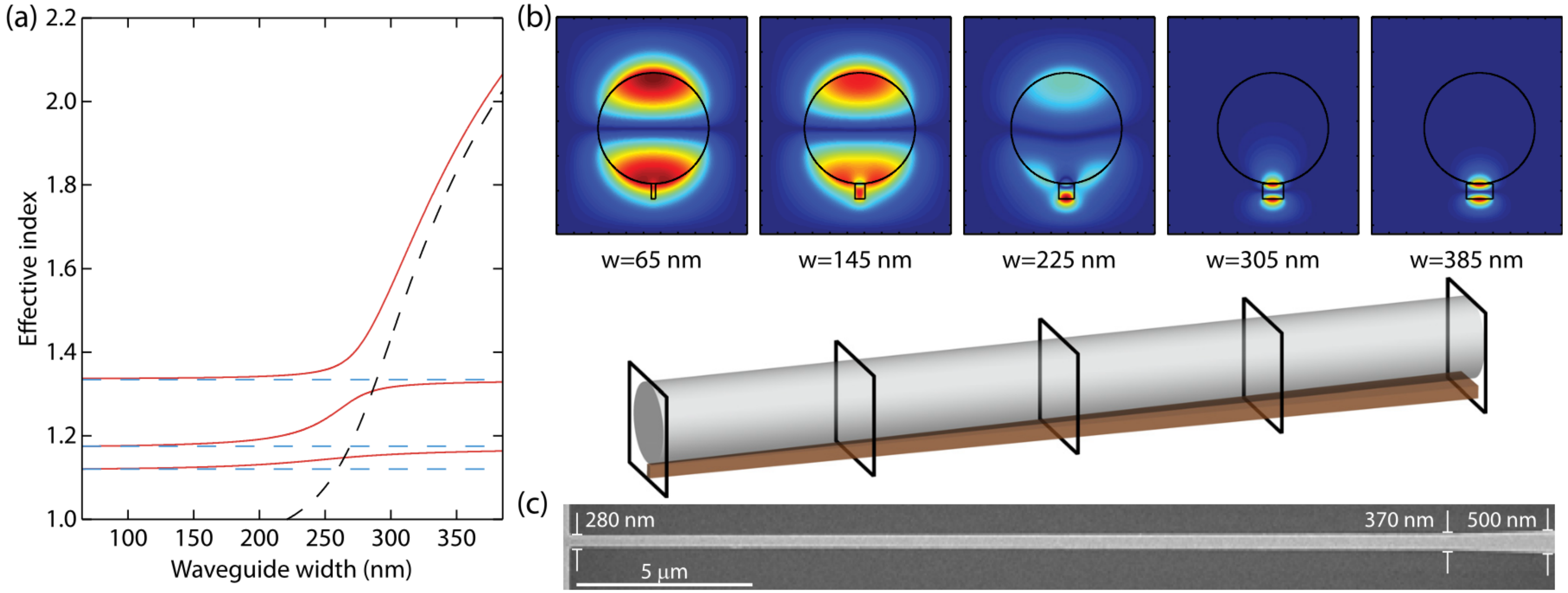

Gröblacher, S., Hill, J. T., Safavi-Naeini, A. H., Chan, J. & Painter, O. Highly efficient coupling from an optical fiber to a nanoscale silicon optomechanical cavity. *Appl. Phys. Lett.* **103**, 181104 (2013).